PROCEEDINGS

MMM 2008

Fourth International Conference

MULTISCALE MATERIALS MODELING

OCTOBER 27-31, 2008 ▪ TALLAHASSEE, FLORIDA, USA

Tackling Materials Complexities via Computational Science

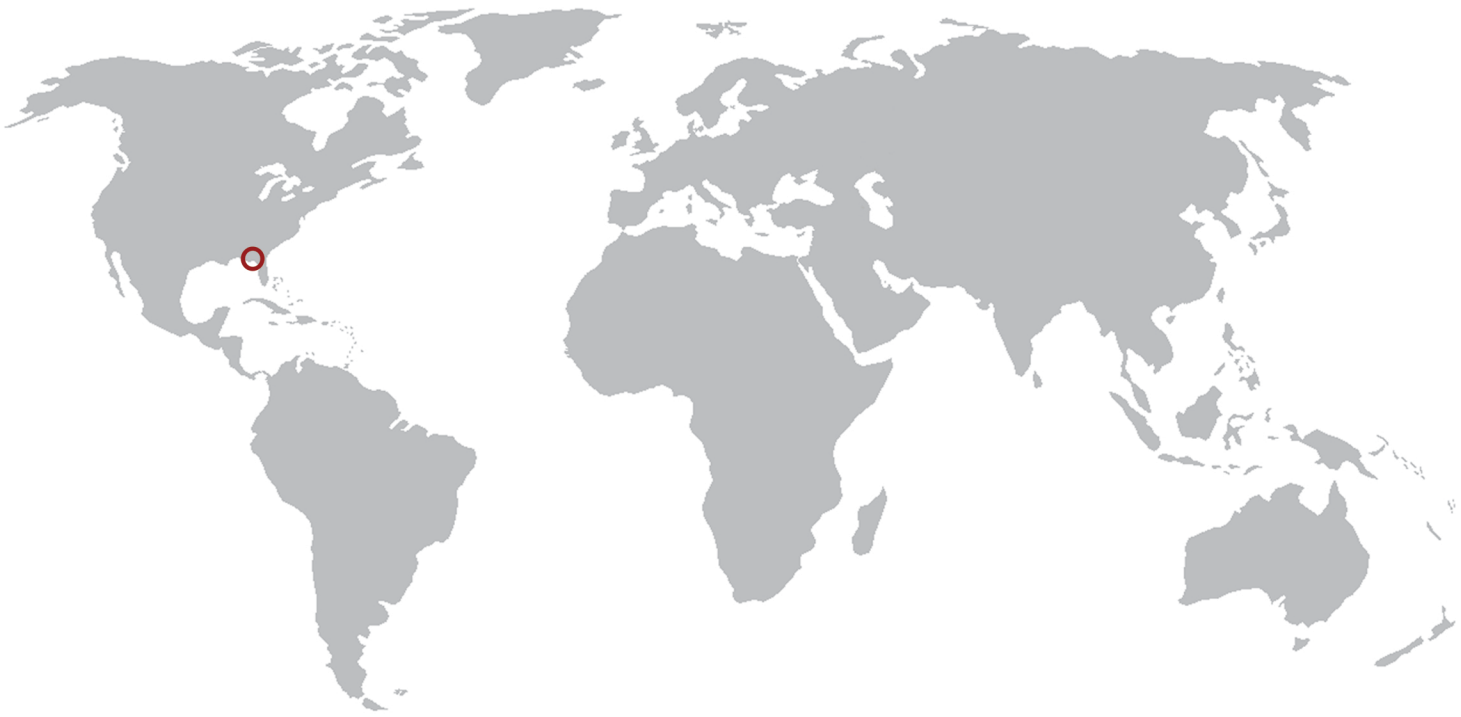

Hosted by the Department of Scientific Computing and Florida State University

DEPARTMENT OF Scientific COMPUTING

FLORIDA STATE UNIVERSITY 1851 VIRES ARTES MORES

Proceedings of

MMM 2008

Fourth International Conference

MULTISCALE MATERIALS MODELING

OCTOBER 27-31, 2008 ▪ TALLAHASSEE, FLORIDA, USA

Anter El-Azab
Editor

Organized and Hosted by
The Department of Scientific Computing and
Florida State University

DEPARTMENT OF Scientific COMPUTING

Papers published in this volume constitute the proceedings of the Fourth International Conference on Multiscale Materials Modeling (MMM-2008). Papers were selected by the program committee for oral or poster presentation. They are published as submitted, in the interest of timely dissemination.

ISBN 978-0-615-24781-6

Department of Scientific Computing
Florida State University
400 Dirac Science Library
P.O. Box 3064120
Tallahassee, FL 32306-4120

Printed in the United States of America

Forward

The field of multiscale modeling of materials promotes the development of predictive materials research tools that can be used to understand the structure and properties of materials at all scales and help us process materials with novel properties. By its very nature, this field transcends the boundaries between materials science, mechanics, and physics and chemistry of materials. The increasing interest in this field by mathematicians and computational scientists is creating opportunities for solving computational problems in the field with unprecedented levels of rigor and accuracy. Because it is a part of the wider field of materials science, multiscale materials research is intimately linked with experiments and, together, these methodologies serve the dual role of enhancing our fundamental understanding of materials and enabling materials design for improved performance.

The increasing role of multiscale modeling in materials research motivated the materials science community to start the Multiscale Materials Modeling (MMM) Conference series in 2002, with the goal of promoting new concepts in the field and fostering technical exchange within the community. Three successful conferences in this series have been already held:

- The First International Conference on Multiscale Materials Modeling (MMM-2002) at Queen Mary University of London, UK, June 17-20, 2002,
- Second International Conference on Multiscale Materials Modeling (MMM-2004) at the University of California in Los Angeles, USA, October 11-15, 2004, and
- Third International Conference on Multiscale Materials Modeling (MMM-2006) at the University of Freiburg, Germany, September 18-22, 2006.

The Fourth International Conference on Multiscale Materials Modeling (MMM-2008) held at Florida State University comes at a time when the wider computational science field is shaping up and the synergy between the materials modeling community and computational scientists and mathematicians is becoming significant. The overarching theme of the MMM-2008 conference is thus chosen to be "*Tackling Materials Complexities via Computational Science*," a theme that highlights the connection between multiscale materials modeling and the wider computational science field and also reflects the level of maturity that the field of multiscale materials research has come to. The conference covers topics ranging from basic multiscale modeling principles all the way to computational materials design. Nine symposia have been organized, which span the following topical areas:

- Mathematical basis for multiscale modeling of materials
- Statistical frameworks for multiscale materials modeling
- Mechanics of materials across time and length scales
- Multiscale modeling of microstructure evolution in materials
- Defects in materials
- Computational materials design based on multiscale and multi-level modeling principles

- Multiscale modeling of radiation effects in materials and materials response under extreme conditions
- Multiscale modeling of bio and soft matter systems

The first five topical areas are intended to cover the theoretical and computational basis for multiscale modeling of materials. The sixth topical area is intended to demonstrate the technological importance and industrial potential of multiscale materials modeling techniques, and to stimulate academia-laboratory-industrial interactions. The last two topical areas highly overlap with the earlier ones, yet they bring to the conference distinct materials phenomena and modeling problems and approaches with unique multiscale modeling aspects.

This conference would not have been possible without the help of many individuals both at Florida State University and around the world. Of those, I would like to thank the organizing team of MMM-2006, especially Professor Peter Gumbsch, for sharing their experience and much organizational material with us. I also thank all members of the International Advisory Board for their support and insight during the early organizational phase of the conference, and the members of the International Organizing Committee for the hard work in pulling the conference symposia together and for putting up with the many organization-related requests. Thanks are due to Professor Max Gunzburger, Chairman of the Department of Scientific Computing (formerly School of Computational Science) and to Florida State University for making available financial, logistical and administrative support without which the MMM-2008 would not have been possible. The following local organizing team members have devoted significant effort and time to MMM-2008 organization: Bill Burgess, Anne Johnson, Michele Locke, Jim Wilgenbusch, Christopher Cprek and Michael McDonald. Thanks are also due to my students Srujan Rokkam, Steve Henke, Jie Deng, Santosh Dubey, Mamdouh Mohamed and Jennifer Murray for helping with various organizational tasks. Special thanks are due to Bill Burgess and Srujan Rokkam for their hard work on the preparation of the proceedings volume and conference program.

I would like to thank the MMM-2008 sponsors: Lawrence Livermore National Laboratory (Dr. Tomas Diaz de la Rubia), Oak Ridge National Laboratory (Dr. Steve Zinkle) and Army Research Office (Drs. Bruce LaMattina and A.M. Rajendran) for the generous financial support, and thank TMS (Dr. Todd Osman) for the sponsorship of MMM-2008 and for advertising the conference through the TMS website and other TMS forums.

I would also like to thank all plenary speakers and panelists for accepting our invitation to give plenary lectures and/or serve on the conference panels. Lastly, I would like to thank the session chairs for managing the conference sessions.

Anter El-Azab
Conference Chair

International Advisory Board

Dr. Tomas Diaz de la Rubia	LLNL, USA
Prof. Peter Gumbsch	Fraunhofer Institute IWM, Freiburg, Germany
Dr. A.M. Rajendran	ARO, USA
Dr. Steve Zinkle	ORNL, USA
Prof. Anter El-Azab	FSU, USA
Prof. Michael Zaiser	Edinburgh, UK
Prof. Xiao Guo	Queens, London, UK
Prof. Shuichi Iwata	University of Tokyo, Japan
Prof. Jan Kratochvil	CTU, Prague, Czech Republic
Prof. Nasr Ghoniem (Chair)	UCLA, USA
Dr. Ladislas Kubin	ONERA-LEM, France
Prof. Shaker Meguid	Toronto, Canada
Prof. Alan Needleman	Brown, USA
Prof. Michael Ortiz	Caltech, USA
Prof. David Pettifor	Oxford, UK
Prof. Robert Phillips	Caltech, USA
Prof. Dierk Raabe	Max Planck Institute, Duesseldorf, Germany
Prof. Yoji Shibutani	Osaka University, Japan
Prof. Subra Suresh	MIT, Massachusetts USA
Prof. Yoshihiro Tomita	Kobe University, Japan
Prof. Erik Van der Giessen	University of Groningen, The Netherlands
Dr. Dieter Wolf	INL, USA
Prof. Sidney Yip	MIT, USA
Prof. David Bacon	Liverpool, UK
Dr. Michael Baskes	LANL, USA
Prof. Esteban Busso	Ecole des Mines, France
Prof. Timothy Cale	RPI, New York, USA
Dr. Moe Khaleel	PNNL, USA
Prof. David Srolovitz	Yeshiva, USA
Prof. Emily Carter	Priceton University, USA
Dr. Dennis Dimiduk	AFRL, USA
Prof. Rich Le Sar	Iowa State University, USA

International Organizing Committee

Weinan E	Princeton University, USA
Max Gunzburger	Florida State University, USA
Mitchell Luskin	University of Minnesota, USA
Rich Lehoucq	Sandia National Laboratories, USA
A.M. Rajendran	U.S. Army Research Office, USA
Stefano Zapperi	University of Rome, Italy
M.-Carmen Miguel	University of Barcelona, Spain
Mikko Alava	Helsinki University of Technology, Finland
Istevan Groma	Eötvös University, Hungary
Tom Arsenlis	Lawrence Livermore National Laboratory, USA
Peter Chung	Army Research Laboratory, USA

Marc Geers	Eindhoven University of Technology, The Netherlands
Yoji Shibutani	Osaka University, Japan
Dieter Wolf	Idaho National Laboratory, USA
Jeff Simmons	Air Force Research Laboratory, USA
Simon Phillpot	University of Florida, USA
Anter El-Azab (Chair)	Florida State University, USA
Daniel Weygand	University of Karlsruhe (TH), Germany
Zi-Kui Liu	Pennsylvania State University, USA
Hamid Garmestani	Georgia Institute of Technology, USA
Moe Khaleel	Pcific Northwest National Laboratory, USA
Mei Li	Ford Motor Company, USA
Fie Gao	Pacific Northwest National Laboratory, USA
Roger Stoller	Oak Ridge National Laboratory, USA
Pascal Bellon	University of Illinois, Urbana-Champaign, USA
Syo Matsumura	Kyushu University, Japan
Jeffery G. Saven	University of Pennsylvania, USA
Wei Yang	Florida State University, USA
T.P. Straatsma	Pacific Northwest National Laboratory, USA
L.P. Kubin	CNRS-ONERA, France
S.J. Zinkle	Oak Ridge National Laboratory, USA
Jaafar El-Awady	University of California, Los Angeles, USA
Shahram Sharafat	University of California, Los Angeles, USA
Hanchen Huang	Rensselaer Polytechnic Institute, USA
Yury N. Osetskiy	Oak Ridge National Laboratory, USA
Ron O. Scattergood	North Carolina State University, USA
Anna M. Serra	Universitat Politecnica de Catalunya, Spain

Local Organizing Committee (Florida State University, USA)

Prof. Anter El-Azab (Chair)
Prof. Max Gunzburger (Co-Chair)
Anne Johnson (Public relations and marketing)
Bill Burgers (Graphics and publications)
Srujan Rokkam (Proceedings and printing)
Michael McDonald (Webmaster)
Michele Locke (Finances)

Sponsors

Special thanks to the following sponsors:

- The Army Research Office
- Lawrence Livermore National Laboratory
- Oak Ridge National Laboratory

for their generous financial support, and to

- The Minerals, Metals & Materials Society (TMS)

for the sponsoring and advertising the conference through the TMS website.

Contents

Symposium 2

Symposium 2

Statistical methods for material deformation and failure

Theory of Nematic and Smectic Elastomers

T.C. Lubensky

Department of Physics and Astronomy, University of Pennsylvania, 209 S. 33rd. Street, Philadelphia, PA 19104-6396
(E-mail: tom@physics.upenn.edu)

ABSTRACT

Liquid crystal elastomers [1] are remarkable materials that exhibit the elastic properties of rubber and the orientational properties of liquid crystals. The coupling between orientation and strain, however, gives rise to properties that are unique to these elastomers. Both nematic and smectic elastomers in their idealized forms are formed via the spontaneous breaking of a continuous rotational symmetry, and, as a result, they exhibit Goldstone modes whose manifestation is the vanishing of certain elastic moduli and soft elastic response in which finite strains can be produced with vanishing stress. Generally the preparation of monodomain samples in the laboratory requires the imposition of a preferred orientation direction via a second crosslinking under uniaxial stress. Samples prepared in this way exhibit semi-soft rather than soft behavior with a nearly flat stress-strain curve for strains between lower and critical values. This talk will introduce a simple model for semi-soft nematic elastomers and discuss its global phase diagram [2], establishing that semi-soft response is associated with the existence of a continuum of equal energy biaxial states. It will also introduce models for smectic elastomers and discuss the unusual nature of soft response that results when a uniaxial smectic-A elastomer undergoes a transition to a biaxial smectic-C elastomer [3]. Finally some comments will be made about the difference between Martensitic and soft or semi-soft response, all of which can occur in liquid crystal elastomers.

[1] M. Warner and E. M. Terentjev, *Liquid Crystal Elastomers* (Oxford University Press, Oxford, 2003).
[2] Fangfu Ye, Ranjan Mukhopadhyay, O. Stenull, and T.C. Lubensky, "Semi-soft Nematic Elastomers and Nematics in Crossed Electric and Magnetic Fields", Phys. Rev. Lett. **98**, 147801/1-4 (2007).
[3] O. Stenull and T.C. Lubensky, "Soft Elasticity in biaxial smectic and smectic-C elastomers", Phys. Rev. E **74**, 051709/1-24 (2006).

This work has been partially supported by the NSF MRSEC (DMR-05-20020) and by NSF Grant DMR 0804900.

Athermal Statistical Mechanics for Material Elastostatics and Deformation

A.H.W. Ngan

Department of Mechanical Engineering, University of Hong Kong, Pokfulam Road, Hong Kong, P.R. China
(Email: hwngan@hku.hk)

ABSTRACT

A stressed solid with random microstructure represents an interesting analogue to a thermal system at equilibrium – the structural randomness qualify for a description by an entropy, and there is also the usual strain energy. Such a system, however, is athermal since the real (Kelvin) temperature can play little role. Instead, an effective temperature θ exists to represent the relative importance of entropy versus energy. Finite-element modeling of the force distribution in stressed low-density elastic networks confirms the existence of such an effective temperature in the description of these structures. The jumpy flow behaviour of materials observed during nanoindentation experiments, and the formation of dislocation patterns in crystals are further examples which can be modelled by the same statistical mechanics framework. A canonical ensemble can also be constructed to calculate the properties of an athermal system.

1. Introduction – "Similarly Random" Structures

This paper deals with the mechanics of materials in which the microstructure is "similarly random". Fig. 1 illustrates a simple example. The network patterns in Fig. 1(a) and (b) are randomly disturbed versions of a regular triangular grid, but these two structures, although different in detail, are rather similar in terms of their overall randomness. On the other hand, the pattern in Fig. 1(c), also a disturbed triangular grid, has evidently very different randomness. One therefore expects the two patterns in Fig. 1(a) and (b) to have similar properties such as overall elastic stiffness or strength, whereas the pattern in Fig. 1(c) should have distinctively different properties.

There are many other materials or structures which are similarly random. The arrangement of grains or beads in a pile under gravity may be random but the randomness may be similar in different locations within the pile. Many natural or biological materials such as wood and trabecular bone also have similarly random microstructures. Synthetic low-density polymeric or metal foams, which find applications in arenas such as tissue engineering, shock absorption or heat transfer, are also examples. The spatial arrangement of microstructures in synthetic materials, such as the patterns of precipitates or dislocations in metals or alloys, may also be similarly random.

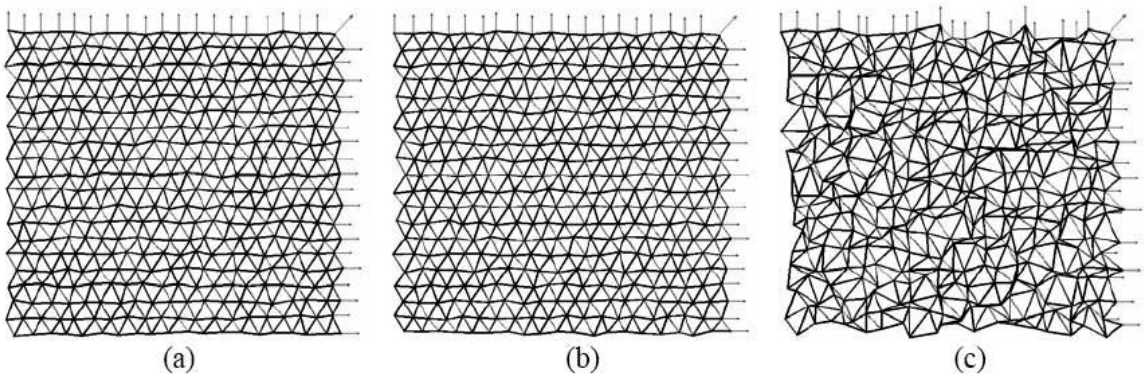

Figure 1. Three computer-generated networks. (a,b) have the same θ value (see text) of 0.5, and (c) has θ value of 10.

Modern materials modelling tools such as finite or discrete element methods, or the newly developed dislocation dynamics method for calculating metal deformation problems, are very powerful, but they are deterministic in nature. While they can be used to calculate one given structure (e.g. Fig. 1(a)) at a time, we do not know whether the properties calculated would apply to a further similarly random structure (e.g. Fig. 1(b)). One indeed expects a particular class of materials, even with similar randomness, to exhibit variations in properties, and so a probabilistic rather than a deterministic description should be used. In this whole argument, one also needs to find a robust way to quantify the randomness of a generic type of structure. For example, when we say the networks in Fig. 1(a) and (b) have the same randomness while that in Fig. 1(c) has a higher randomness, what exactly do we mean by that?

The aim of the present paper is to summarize the author's recent work on the above issues. The central idea is to use statistical mechanics concepts to provide the probabilistic description needed. However, the scope is limited to properties that are athermal, i.e. not affected by thermal effects. As such, the aim is not a theory for glass or amorphous materials, which has to focus on the random arrangement of the individual atoms. The focus here is on microstructures that are much larger than atomic scale so that they exhibit degrees of freedom which are decoupled from atomic vibrations. For example, the straining of the struts in the networks in Fig. 1 when the latter are stretched should be athermal as long as the stretching is done in a quasi-static manner.

2. Athermal Entropy and Temperature

2.1 Elastic Networks

Consider a very large network, such as one of those shown in Fig. 1. Due to the structural randomness, an athermal entropy S can always be defined. Suppose $P(f)$ is the distribution of the force f in the struts, S can be defined as

$$S = -\int_{-\infty}^{\infty} P(f)\ln[P(f)]df\,. \tag{1}$$

Each force f produces a work done $W(f)$, and so the energy of the network is given by

$$U = \int_{-\infty}^{\infty} W(f)\, P(f) df \,. \tag{2}$$

At equilibrium U should be minimized, but since a given structural randomness is to be maintained, S should be constrained. The problem thus becomes the variational principle of minimizing the free energy $F = U - \theta S$, i.e.

$$dF = dU - \theta\, dS = 0 \tag{3}$$

where θ is mathematically a Lagrange multiplier and physically a temperature-like quantity, albeit the fact that it has nothing to do with the real Kelvin temperature T of the network.

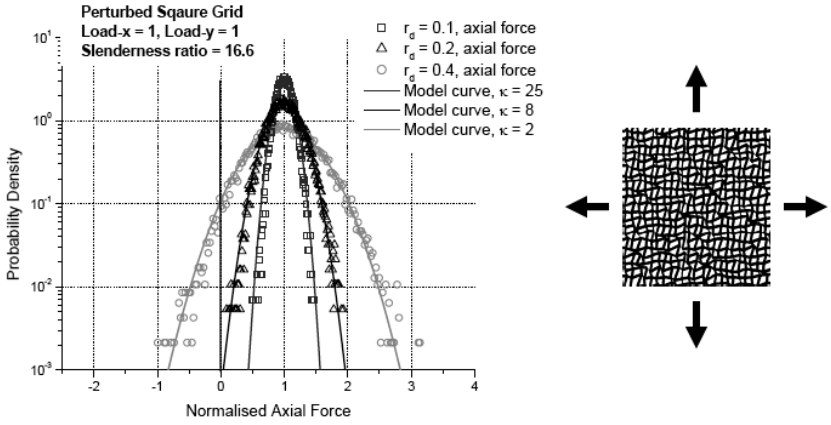

Figure 2. Axial force distribution of 2-D perturbed networks under hydrostatic loading [1,2].

The point symbols in Fig. 2 are finite-element (FE) calculations of the axial force distribution of a series of 2-D strut networks constructed with different randomness [1,2]. The randomness here is defined by a quantity r_d, where $r_d = 0$ corresponds to a regular square network, and a network with $r_d > 0$ is constructed by randomly displacing each grid point of the square network within a region $(r_d L) \times (r_d L)$, where L is the periodic spacing in the regular pattern. The randomness of the network thus constructed increases with r_d, and the example shown on the right side of Fig. 2 has an r_d value of 0.4. It can be seen that the FE calculated force distribution becomes more spread as the structural randomness increases, as expected. The curves in Fig. 2 are the theoretical results from eqn. (3). Such a variational procedure leads to a family of $P(f)$ curves each characterized by a specific value of θ. κ in Fig. 2 is an inverse measure of the athermal temperature θ, and it can be seen that by choosing a correct value of θ or κ, excellent matching

with the FE results can be obtained. The theory involving eqn. (3) is thus verified. The contact force distribution in granular packings has also been studied using a similar approach [1,2].

2.2 Plasticity Phenomena

Plasticity usually occurs in sporadic bursts with random sizes in the sub-micron range. A number of reports have indicated that the burst size Ψ follows scale-free statistics, but for confined situations such as nanoindentation, large bursts are unlikely to occur out of the very small deformation zone, and experiments have shown that the burst size in this case tends to follow scale-limited statistics of the form $P(\Psi) \sim \exp(-k\Psi)$ [3], see Fig. 3(a). This exponential form of $P(\Psi)$ is consistent with a maximum entropy principle, where $S = -\int P(\Psi)\ln[P(\Psi)]d\Psi$, subject to the condition that the mean burst size $\overline{\Psi} = \int \Psi P(\Psi) d\Psi$ is fixed.

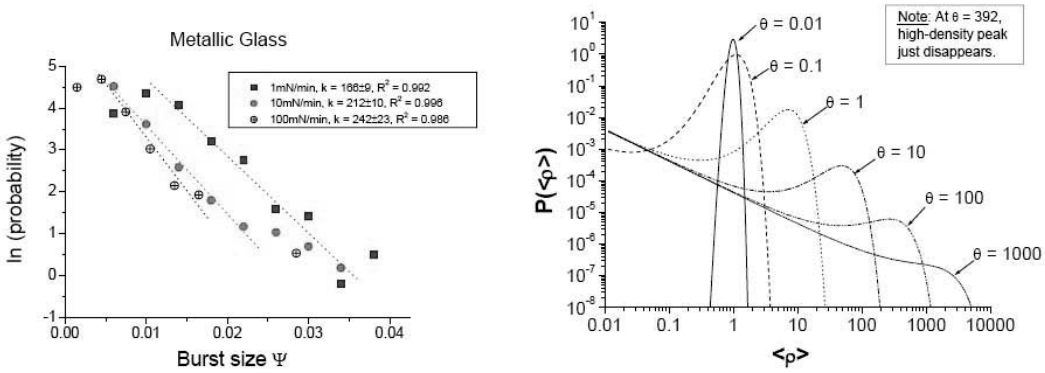

(a) (b)

Figure 3. (a) Occurrence statistics of strain bursts during nanoindentation of a Zr-based metallic glass by a micron-sized indenter [3]. (b) Predicted probability distribution of dislocation density at various θ values [4].

A further example where statistical mechanics may be applicable is the formation of dislocation patterns during crystal plasticity. In this case, the mutual interaction of dislocations in a pattern constitutes an energy functional of the dislocation density function ρ which describes the pattern. When ρ is small, an approximate form for this energy functional is [4]:

$$U = \frac{1}{\overline{\rho}} \int_0^\infty E\,\rho\,P_e(E)\,dE \quad + \quad E_o, \qquad \text{where} \quad E(\rho) \approx \frac{\alpha\mu b^2}{4} \ln\left(\frac{\rho}{\rho_{\min}}\right), \tag{4}$$

E_o is a constant, $\rho_{\min}$ corresponds to the outer cut-off distance, $\alpha \approx 1$, μ is shear modulus and b Burgers vector. Entropy is $S = -k \int P_e(E) \ln\left[P_e(E)\right] dE$, and because $P(\rho) = (\alpha\mu b^2 / 4\rho) P_e(E)$, eqn. (3) leads to

$$P(\langle\rho\rangle) = \frac{A}{\langle\rho\rangle} \exp\left[\frac{\langle\rho\rangle}{\theta}\left(c - \ln\langle\rho\rangle\right)\right], \tag{5}$$

where $<\rho>=\rho/\overline{\rho}$ is the dislocation density normalized by the mean value, and A and c are normalizing constants. Fig. 3(b) shows plots of eqn. (5) at different θ values. As very low values (e.g. 0.01) of θ, which represents noise in the system, $P(\rho)$ is singlely peaked at the mean density value, indicating a homogeneous distribution of dislocations. At intermediate values of θ, $P(\rho)$ becomes bimodal with peaks at a high and a low density, corresponding to cellular patterning. At high values of θ (> 392), the high-density peak disappears and $P(\rho)$ becomes power-law distributed, indicating fractal patterning. Different types of patterning are thus predicted depending on the noise level.

3. Constant-(N,V,T,θ) Ensemble within Harmonic Approximation

Within the harmonic approximation, it is always possible to write the Hamiltonian H of a solid as two independent thermal and mechanical components, i.e. $H = H_{therm} + H_{mech}$, where H_{therm} and H_{mech} can accept any energy value without affecting one another. An ensemble of A such solids is therefore a dual-bath ensemble shown in Fig. 4, where the thermal and the mechanical components do not interact, i.e. each system accepts a mechanical and a thermal component of energy, separately drawn from the pools of $A\overline{E}_{mech}$ and $A\overline{E}_{therm}$ respectively, where $\overline{E}_{mech}$ and $\overline{E}_{therm}$ are the average mechanical and thermal energies per system. It follows that the total entropy of the ensemble is $S_{ens} = S_{therm} + S_{mech}$ where S_{therm} and S_{mech} do not interact. Applying the First Law to the ensemble, any heat flow dQ into the ensemble interacts with S_{therm} only, and any external mechanical work dU on the ensemble interacts with S_{mech} only. As a result, the equilibrium conditions are given separately by:

$$dQ - T\,dS_{therm} = 0 \qquad \text{and} \qquad dU - \theta\,dS_{mech} = 0\,. \tag{6}$$

The second condition above is the ensemble version of the equilibrium condition in eqn. (3), and it enables the mechanical temperature θ to be defined properly. Since all ensembles with the same average strain energy $\overline{E}_{mech}$ per system are characterized by the same θ, and systems can have the same average strain energy, when subject to the same external conditions, only if they have the same structural randomness, θ is therefore an indicator for structural randomness, i.e. two systems have the same θ if their structures are similarly random. As an example, the network patterns in Fig. 1 were generated by a Monte Carlo scheme consistent with the constant-(N,V,θ) ensemble discussed here. This ensemble approach has also been applied to investigate dislocation patterning behaviour [5].

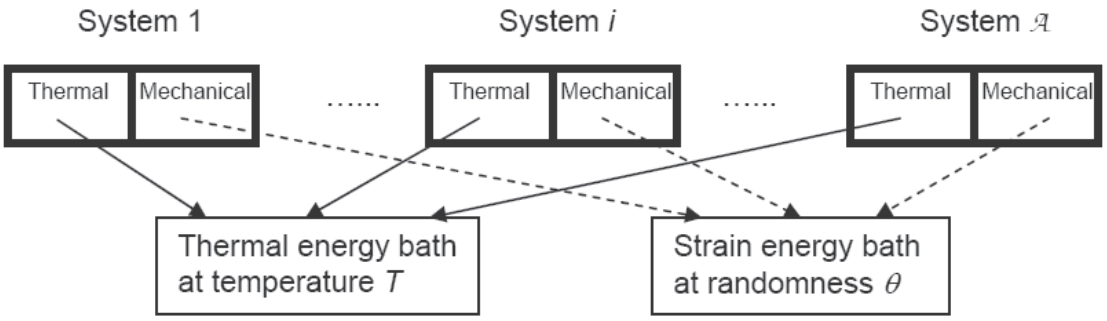

Figure 4. Dual-bath ensemble

4. Conclusions

An athermal statistical mechanics framework has been proposed to model the mechanics of materials with random microstructures. This is applicable to model the elastostatics of random structures, as well as to discrete plasticity phenomena.

Acknowledgement

The work described here was supported by a grant from the Research Grants Council of the Hong Kong Special Administrative Region, P.R. China (Project No.HKU7156/08E).

References

[1] A.H.W. Ngan, "On the Distribution of Elastic Forces in Disordered Structures and Materials – Part I: Computer Simulation", Proceedings of the Royal Society of London Ser. A, **461**, 433 (2005).

[2] A.H.W. Ngan, "On the Distribution of Elastic Forces in Disordered Structures and Materials – Part II: A Statistical Mechanics Theory", Proceedings of the Royal Society of London Ser. A, **461**, 1423 (2005).

[3] H. Li, A.H.W. Ngan, M.G. Wang, "Continuous Strain Bursts in Crystalline and Amorphous Metals during Plastic Deformation by Nanoindentation", Journal of Materials Research, **20**, 3072 (2005).

[4] A.H.W. Ngan, "Dislocation patterning – a statistical mechanics perspective", Scripta Material, **52**, 1005 (2005).

[5] A.H.W. Ngan, R. Thomson, "Nonequilibrium statistical mechanics of the evolution of a dislocation structure", Physical Review B, **75**, 014107 (2006).

Mesoscopic description of martensitic phase transformations mediated by dislocations using the Landau-Ginzburg theory

Authors: Roman Gröger, Turab Lookman, Avadh Saxena

Affiliations: Statistical Physics and Condensed Matter Group and Center for Nonlinear Studies, Theoretical Division, Los Alamos National Laboratory, MS B258, Los Alamos, NM 87545. groger@lanl.gov

ABSTRACT

Dislocations in crystals induce incompatibility between elastic strains. We show how this can be related to the densities of crystal dislocations in individual slip systems and how the incompatibility causes nonlocal coupling with elastic strains in the evolving microstructure. The order parameter and thus the corresponding stress fields develop long-range tails that correspond to the superposition of elastic stress fields of individual dislocations. Hence, the stress field of any distribution of dislocations in an arbitrarily anisotropic medium can be calculated just by minimizing the free energy. The corresponding continuous field of Peach-Koehler forces is then employed in a Fokker-Planck equation for the dynamics of the dislocation density. This approach represents a simple self-consistent scheme that yields the evolutions of both the order parameter field and the continuous dislocation density.

1 Introduction

A mesoscopic description (nano to micrometer) of physical processes in solids, where atomic length scales merge with those of the continuum, represents a crucial and perhaps most challenging aspect of understanding material behavior. This arises, for example, during displacive (martensitic) phase transformations where the distortions associated with the strains in unit cells and intra-unit cell displacements (or shuffles) propagate over larger distances so that competing long-range effects lead to the formation of inhomogeneities such as interfaces, spatially correlated domains and complex microstructure. The currently available mesoscopic models for studies of defects focus mainly on the self-organization of dislocations in spatially homogeneous microstructures. The statistical models based on the Fokker-Planck equation have been pioneered by Bakó and Groma [1] and Zaiser [2]. A closer connection with the well-established Kröner's continuum theory of dislocations [3] was developed by El-Azab [4] and the formation of sharp dislocation walls in isotropic media was observed by Limkumnerd and Sethna [5]. Phase field models of dislocation patterning are usually based on the theory of Khachaturyan [6] where the dislocation loops are viewed as coherent platelet inclusions.

Our objective in this paper is to incorporate dislocations into the Landau theory to study martensitic phase transformations in materials containing defects. We consider an anisotropic medium that is described by the elastic constants corresponding to the high-temperature cubic phase. Utilizing Kröner's continuum theory of dislocations [3], we develop a self-consistent scheme that allows simultaneous calculation of the microstructure and the evolution of the dislocation density.

2 Free energy for materials with dislocations

In the following we will consider a square to rectangle phase transformation, where the square corresponds to the austenite phase stable above T_c and the two variants of the rectangle to the martensite that is stable below T_c. We identify three order parameters e_1, e_2 and e_3 that correspond to the three modes of in-plane deformation of the reference square lattice. In particular, $e_1 = (\varepsilon_{11} + \varepsilon_{22})/\sqrt{2}$ measures isotropic dilation, $e_2 = (\varepsilon_{11} - \varepsilon_{22})/\sqrt{2}$ the change of shape and $e_3 = \varepsilon_{12}$ the change of right angles caused by the shear. For the square to rectangle transformation, e_2 is the primary order parameter and e_1, e_3 are secondary order parameters.

The nonzero plastic strains induced by the dislocations cause discontinuities in the displacement field and these are removed by elastic relaxation. The elastic components of the strain tensor are then incompatible with each other and are constrained by $\nabla\times\nabla\times\boldsymbol{\varepsilon} = \boldsymbol{\eta}$, where $\boldsymbol{\eta}$ is the so-called incompatibility tensor. In the two-dimensional case, the only scalar equation that is not satisfied identically reads $\partial_{22}\varepsilon_{11} - 2\partial_{12}\varepsilon_{12} + \partial_{11}\varepsilon_{22} = \eta_{33}$, where $\partial_{ij} \equiv \partial^2/\partial x_i \partial x_j$. Writing the strains in terms of the order parameter fields then yields the incompatibility constraint for the order parameters:

$$\nabla^2 e_1 - (\partial_{11} - \partial_{22})e_2 - \sqrt{8}\partial_{12}e_3 = \eta_{33}\sqrt{2} \quad . \tag{1}$$

The Landau free energy for the martensitic phase transformations is typically constructed using the harmonic term that follows from the elastic strain energy (terms with e_1^2, e_2^2, e_3^2) augmented by even higher-order terms of e_2 that are allowed by symmetry, and by a gradient term proportional to $|\nabla e_2|^2$ which accounts for the energy cost for spatial variation of the order parameter [7]. Writing (1) as $G = 0$ we include the incompatibility constraint using the Lagrange multiplier λ as

$$F = \int_S \Big[\underbrace{\frac{A_2}{2}e_2^2 + \frac{B}{4}e_2^4 + \frac{C}{6}e_2^6}_{f_{loc}} + \underbrace{\frac{A_1}{2}e_1^2 + \frac{A_3}{2}e_3^2}_{f_{nonloc}} + \underbrace{\frac{K_2}{2}|\nabla e_2|^2}_{f_{grad}} + \lambda G \Big] \mathrm{d}\mathbf{r} \quad . \tag{2}$$

The problem is to calculate the primary order parameter e_2 and the incompatibility field η_{33} (i.e. the dislocation density) that minimize the free energy (2). Firstly, we look for the minimum of F with respect to the secondary order parameters e_1, e_3 and the Lagrange multiplier λ. The stationarity conditions $\delta F/\delta e_1 = \delta F/\delta e_3 = \delta F/\delta\lambda = 0$ yield e_1 and e_3 as functionals of e_2 and η_{33}. By substituting these back into (2) the free energy only depends on e_2 and η_{33}.

In the Kröner's continuum theory of dislocations [3], the incompatibility tensor is defined as $\boldsymbol{\eta} = \mathrm{sym}\,(\nabla\times\boldsymbol{\alpha})$, where $\boldsymbol{\alpha}$ is the Nye tensor with components $\alpha_{ij} = B_j/S_i$. Here, $\mathbf{B}$ is the so-called net Burgers vector that is obtained as a vector sum of the Burgers vectors of all crystal dislocations that comprise the mesoscopic cell perpendicular to x_i with area S_i. In our two-dimensional case,

$$\eta_{33} = \alpha_{32,1} - \alpha_{31,2} \tag{3}$$

and, therefore, only edge dislocations with their line directions parallel to x_3 and the Burgers vector components along x_1 and x_2 contribute to this incompatibility. Although the incompatibility (3) is completely determined by the distribution of the net Burgers vectors $\mathbf{B}$, a connection still needs to be made between $\mathbf{B}$ and the density of crystal dislocations that populate individual slip systems. Due to the mesoscopic nature of this model, we cannot invoke individual crystal dislocations but will merely consider their densities in each slip system. This is accomplished by writing

$$\alpha_{3i} = B_i/S_{cell} = \sum_s (n^{s+} - n^{s-})b_i^s \quad , \tag{4}$$

where S_{cell} is the area of one mesoscopic cell, the sum is over all the slip systems s, and n^{s+} and n^{s-} are non-negative densities of crystal dislocations with the Burgers vectors $\mathbf{b}^s$ and $-\mathbf{b}^s$, respectively. Substituting (4) into (3) yields the sought after connection between the densities of crystal dislocations and the mesoscopic incompatibility field:

$$\eta_{33} = \epsilon_{ij} \sum_s \frac{\partial (n^{s+} - n^{s-})}{\partial x_i} b_j^s \quad , \tag{5}$$

where ϵ_{ij} is the antisymmetric Levi-Civita tensor.

We can now proceed to construct a numerical scheme that will minimize the free energy (2) subject to finite dislocation densities n^{s+} and (or) n^{s-}. We will assume that the time scale of relaxation of the order parameter is much shorter than that of the dislocation density. The relaxation of the order parameter field will then be accomplished by the relaxational dynamics

$$\frac{\partial e_2}{\partial t} = -\Gamma \frac{\delta F}{\delta e_2} \quad , \tag{6}$$

where Γ is the mobility coefficient, and during this relaxation we keep the dislocation density fixed. From the relaxed order parameter field we can calculate the strain field and, using the Hooke's law, also the internal stress field. Hence, the components of the Peach-Koehler forces on the dislocations in each mesoscopic cell can be calculated as $F_k^{s\pm} = \mp \epsilon_{jk} \sigma_{jl} b_l^s$ and the corresponding glide component, $\mathbf{F}_{glide}^{s\pm}$, by projecting the former into the individual slip systems s. In order to conserve the total Burgers vector in the simulated domain, the dislocation densities are evolved using the Fokker-Planck equations

$$\frac{\partial n^{s\pm}}{\partial t} = -D \nabla \cdot [\mathbf{F}_{glide}^{s\pm} n^{s\pm}] \quad . \tag{7}$$

The individual dislocation densities are propagated through the time step Δt and the corresponding new incompatibility field is obtained from (5). In the next step we utilize (6) to calculate the order parameter field e_2 that minimizes the free energy subject to this new incompatibility field. This recursive procedure represents a simple self-consistent scheme for a simultaneous calculation of the microstructure and the dislocation density.

3 Simulations

We will now utilize the procedure outlined above to study the self-organization of dislocations in a single crystal of Fe-30at.%Pd below T_c. The simulated domain consists of 128×128 mesoscopic unit cells, each containing 1000×1000 crystallographic unit cells with the lattice parameter 3.8 Å. Hence, the width of the simulated domain is 48.64 μm. In this material the crystal dislocations responsible for accommodating plastic strain are those with the Burgers vectors $1/2\langle 110 \rangle$, i.e. in our two-dimensional case we consider two slip systems, with the Burgers vectors of the dislocations $\pm 1/2[110]$ and $\pm 1/2[\bar{1}10]$. To each mesoscopic cell we initially assign a dislocation density that is drawn at random from a uniform distribution; this yields the density $\rho = 2 \times 10^{14}$ m^{-2}.

During the minimization the initially spatially uniform dislocation density (Fig. 1a) rapidly develops alternating dislocation walls that decorate the twin boundaries between different variants of the martensite (Fig. 1b). This is shown more clearly in the field of the net Burgers vectors

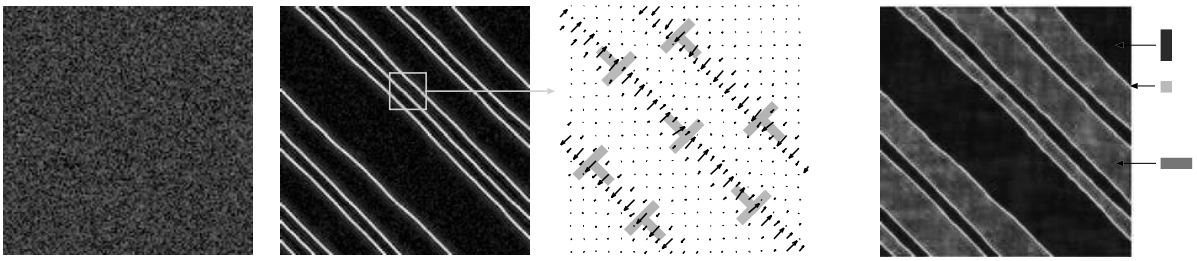

(a) (b) (c) (d)

Figure 1: Initial (a) and final (b) density of dislocations, where dark regions correspond to low and bright regions to high $|\mathbf{B}|$, respectively. The final field of net Burgers vectors $\mathbf{B}$ is shown in (c). The final field e_2 is shown in (d), where blue and red correspond to the two variants of the martensite and the twin boundaries to the metastable austenitic phase.

in Fig. 1c. The microstructure (i.e. the order parameter field) corresponding to the dislocation density in Fig. 1b,c exhibits well-defined twins corresponding to the two variants of the martensite (Fig. 1d) separated by twin boundaries.

4 Conclusions

The Landau theory outlined in this paper represents the first step in the formulation of a mesoscopic theory for studying martensitic phase transformations mediated by defects. In the framework of Kröner's theory [3] utilized here, the dislocations induce incompatibility between the components of the elastic strain tensor. The "strength" of this incompatibility is related to the densities of crystal dislocations in individual discrete slip systems. The coupling between the order parameter field and the dislocation density introduces competition and frustration in the evolving microstructure and, therefore, the minimization of the free energy is accomplished simultaneously by the order parameter field and the dislocation density. This results in formation of correlated dislocation walls at the twin boundaries. The detailed explanation of this model can be found at `arXiv:0806.4564`.

References

[1] B. Bakó and I. Groma. Stochastic approach for modeling dislocation patterning. *Phys. Rev. B*, 60(1):122–127, 1999.

[2] M. Zaiser. Scale invariance in plastic flow of crystalline solids. *Adv. Phys.*, 55(1-2):185–245, 2006.

[3] E. Kröner. *Continuum theory of dislocations and self-stresses*. Springer-Verlag, 1958.

[4] A. El-Azab. The boundary value problem of dislocation dynamics. *Model. Simul. Mater. Sci. Eng.*, 8:37–54, 2000.

[5] S. Limkumnerd and J. Sethna. Mesoscale theory of grains and cells: Crystal plasticity and coarsening. *Phys. Rev. Lett.*, 96:095503, 2006.

[6] A. G. Khachaturyan. *Theory of structural transformations in solids*. J. Wiley & Sons, 1983.

[7] S. R. Shenoy, T. Lookman, A. Saxena, and A. R. Bishop. Martensitic textures: Multiscale consequences of elastic compatibility. *Phys. Rev. B*, 60(18):R12537–12541, 1999.

Heterogeneous Dynamics Near Dislocation Jamming

Lasse Laurson[1], M.-Carmen Miguel[2], and Mikko J. Alava[1]

[1]Department of Engineering Physics, Helsinki University of Technology, P.O. Box 1100, 02015 HUT, Finland
[2]Departament de Física Fonamental, Facultat de Física, Universitat de Barcelona, Diagonal 647, 08028 Barcelona, Spain.
(E-mails: lla@fyslab.hut.fi, carmen.miguel@ub.edu, mja@fyslab.hut.fi)

ABSTRACT

Jamming is a transition at which constituent particles of a system stop collectively their movement. Experimental observations on a broad class of systems ranging from granular media to supercooled liquids show that their dynamics becomes increasingly heterogeneous when approaching the jamming transition. This is achieved by tuning a control parameter such as temperature, density or the external drive rate. To quantify such dynamics, various methods have been introduced in the literature including e.g. the dynamic four-point susceptibility $\chi_4(1,\tau)$, characterizing correlations across intervals of both space and time.

Dislocation assemblies in plastically deforming crystals with an external stress as a control parameter exhibit some of the typical characteristics of a jamming transition, such as slow dynamics and scaling features near the jamming threshold. Qualitatively, this can be understood to result from a combination of kinetic constraints on dislocation motion due to the underlying crystal structure and long range anisotropic interactions between dislocations, which together induce metastable jammed dislocation configurations.

Here, we explore further the analogy between simple two-dimensional dislocation ensembles and other systems exhibiting jamming, by considering the mean square dislocation displacement, the dynamic four point susceptibility $\chi_4(1,\tau)$, as well as the displacement distribution as a function of a observation time interval τ. Our results on the behavior of $\chi_4(1,\tau)$ point towards the existence of a growing dynamic correlation length as the jamming threshold is approached within the moving phase. Moreover, the displacement distributions of the dislocations seem to be characterized by exponential tails, similarly to many other systems with glassy dynamics.

Topology and Transport in Driven Vortex Lattices

Paolo Moretti and M. Carmen Miguel

Departament de Fisica Fonamental, Universitat de Barcelona
Marti i Franques 1, Barcelona E-08028 Spain
(E-mail: paolo.moretti@ub.edu)

ABSTRACT

Recent studies have established a tight connection between driven vortex lattices in Type II superconductors and plastically deforming crystals. Both the atomistic and the mesoscopic behavior of disordered vortex assemblies under the effect of applied external currents implies topological rearrangements which involve dislocations and dislocation assemblies and result in the emergence of polycrystalline and amorphous states. In this work we emphasize the close relation between topological adjustments of the vortex lattice and its electrodynamic response. We performed a numerical study of the critical current as a function of the defect density and the number of vortices. For weak pinning interactions, the dynamics of dislocation assemblies is the relevant mechanism that accounts for the collective motion of the vortex array.
Dislocations rearrange into grain boundaries, leading to the emergence of polycrystalline order. We prove that grain boundary interactions with defects are responsible for a non-trivial dependence of critical currents on the average defect density and we are able to corroborate previous analytical results that predicted the transition between individual and collective pinning regimes. Vortex flow exhibits typical fingerprints of collective dislocation dynamics, such as *1/f* noise voltage response and history dependence.

1. Introduction

A great deal of attention has been recently devoted to the topology of defected vortex lattices in type II superconductors and the role of topological defects, such as dislocations, in the emergence of disordered phases and critical current anomalies. It is well known that magnetic fields penetrate samples of type II superconductors in the form of quantized flux lines, referred to as vortices, which would arrange themselves into ordered quasi two-dimensional lattices and move under the action of Lorenz-like forces induced by external currents [1]. Quenched disorder and thermal fluctuations tend to break long-range order giving rise to disordered phases. The loss of topological order is envisaged as the main responsible for abrupt variations in the critical current of the driven vortex array.

In the following, we propose a numerical study of the interplay of topology and current transport in type II superconductors. We simulate driven vortex polycrystals and assess the relevance of

dislocation dynamics to vortex motion and their coupling to quenched disorder. In the case of weak pinning interactions, the dynamics of dislocation assemblies proves the relevant mechanism that accounts for the anomalous response to an applied current.

2. Numerical method and simulation technique

Transport properties in our simulations are quantified by looking at the critical current J_c of the vortex array. Topology can be taken care of at any time step by means of Delaunay triangulations and diffraction patterns. We simulate vortex dynamics in the presence of an external current by numerical integration of the set of Langevin equations:

$$\Gamma\, d\mathbf{r}_i/dt = \Sigma_{ij}\, \mathbf{f}_{vv}(\mathbf{r}_i - \mathbf{r}_j) + \Sigma_{ij}\, \mathbf{f}_{vp}(\mathbf{r}_i - \mathbf{r}_j) + \Sigma_{\mathrm{i}}\, \mathbf{f}_L(\mathbf{r}_i) \quad (1)$$

where Γ is the effective viscosity of vortex flow, $\mathbf{f}_{vv}$ is the vortex mutual interaction force according to the London description of the array, $\mathbf{f}_{vp}$ the pinning force exerted by each of the N_p randomly distributed pinning points as derived from a gaussian potential of range ξ (corresponding to the coherence length of the superconducting state), and $\mathbf{f}_L$ the Lorenz force associated with the external current. Integration is performed with an adaptive-step-size fifth-order Runge-Kutta algorithm, imposing periodic boundary conditions in 2D space. We consider a 2D superconducting cross section of fixed linear dimension, perpendicular to the external magnetic field **B** along the z direction, where we locate a set of N_v rigid and interacting vortices and the N_p fixed and randomly distributed pinning points.

Critical currents are recorded as a function of N_p, for different values of the number of vortices N_v, which measures the stiffness of the array. Measurements are performed starting from two different initial configurations, a vortex polycrystal and a perfect (dislocation-free) vortex lattice. The vortex polycrystal is obtained by relaxation of a random vortex array. The system recrystallizes until pinning forces start counteracting grain growth. This protocol is experimentally known as *field-cooling*, as it corresponds to a rapid quench of a high temperature phase. Vortices remain frozen in a metastable polycrystalline state, where dislocations are mainly arranged in low-angle grain boundaries. When starting from a dislocation-free lattice, instead, we simulate what is known as a *zero field-cooling* experiment. Our aim is to assess the role of dislocation arrays in the nonlinear response of the vortex lattice (depinning transition) by comparing results obtained for the two different initial conditions.

3. Results and discussion

Dislocation assemblies prove to affect the nature of the critical response of the system in a dramatic way. In dislocation-free lattices, the vortex array starts moving collectively as the critical current is reached and its behavior is that of a driven elastic system, close to a continuous transition. This is known as elastic depinning of the vortex lattice. By letting the system build up dislocations, instead, we recreate what is known in experiments as plastic depinning. Close to the threshold, the dynamics is highly heterogeneous, meaning that due to the complexity of

dislocation interactions, certain regions show higher mobility, while others remain dynamically frozen.

Critical current as a function of the pinning density is shown in Fig.1. We observe that the dependence on N_p matches the predictions (provided in previous studies [2]) for individual grain boundary pinning at low defect density and collective grain boundary pinning at high defect density. By increasing the defect density, the response switches from a linear growth (in a region where the grain sizes decrease rapidly as N_p is increased) to a square root behavior (where grain sizes stop decreasing, or equivalently the number of dislocations stops increasing). In order to validate the theory of GB pinning, we observe that the critical current for a driven vortex crystal shows no crossover behavior instead. It is indeed a well-established result that, in the absence of dislocations, pinning of vortex lattices is only collective, for weak enough pinning forces [3].

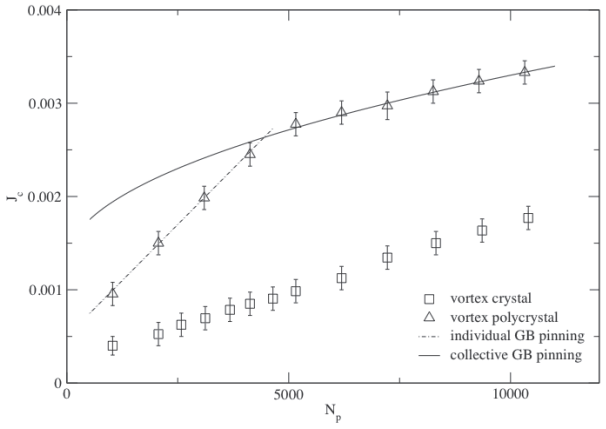

Figure 1. Critical current as a function of the number of defects, as obtained for a vortex polycrystal and a vortex crystal, for N_v=3120 vortices. Numerical results are compared to theoretical predictions for grain boundary pinning.

This proves that GB pinning is essential to explain the dynamics of a vortex polycrystal and that plastic depinning can hardly be understood without accounting for the collective nature of dislocation dynamics. A further confirmation comes from the scaling of critical currents with the number of vortices N_v. Simple arguments suggest the relation $J_c=\alpha\ N_p/N_v$ for individual GB pinning [2], where α is a constant. This result is recovered in our simulations, as reported in Fig. 2.

For a vortex polycrystal, the nature of the depinning transition switches to weakly discontinuous, in analogy with what is observed in disordered colloidal crystals [4]. Close to depinning, dislocations are created and annihilated at the same rate and no healing is observed. Under these conditions, we recorded that vortex flow in the steady state is associated with features such as *1/f* noise in the voltage response (collective vortex velocity), a fingerprint of collective dislocation dynamics [5], as opposed to the washboard peaks observed in driven dislocation-free lattices [6]. By increasing the applied current, dislocation densities change (eventually leading to healing for very high currents and weak enough disorder) and hysteretic behavior can be spotted by ramping

the current up and down above depinning. In fact, dislocation densities affect the magnitude of critical currents. Unlike a perfect crystal, a dislocated lattice owns a much larger number of degrees of freedom and adapts better to disorder, leading to a higher J_c (see Fig. 1). It is thus inevitable that a partial healing at high currents results in a lowered J_c and consequently in history dependence and hysteresis. We also observed that for much higher disorder strengths, the loss of topological order is such that critical currents exhibit a sharp jump as the defect density is increased. The depinning transition becomes strongly discontinuous and the steady state dynamics highly heterogeneous. Vortex flow proceeds in a channel like fashion and high drive healing is replaced by a smectic phase. This novel regimes is currently a matter of investigation.

4. Conclusions

We have performed numerical simulations of driven vortex polycrystals. The presence of dislocation assemblies proved essential to explain the nature of the steady state of vortex flow and the dependence of the critical current on disorder. The loss of topological order is accompanied by a significant increase in the critical current and several features such as history dependence broadband voltage noise find a natural explanation in dislocation dynamics.

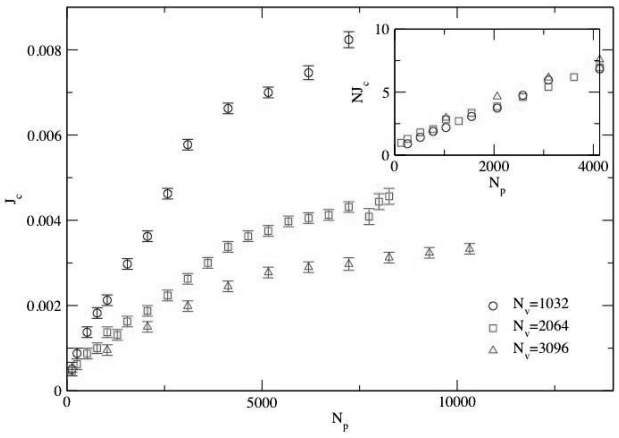

Figure 2. Scaling of the critical current as a function of the number of vortices N_v.

References

[1] G. Blatter *et al.*, Rev. Mod. Phys. **66**, 1125 (1994)
[2] P. Moretti *et al.*, Phys. Rev. B **69**, 214103 (2004), Phys. Rev. Lett. **92**, 257004 (2004), Phys. Rev. B **72**, 014505 (2005)
[3] T. Giamarchi and P. Le Doussal, Phys. Rev. B **52**, 1242 (1995)
[4] A. Pertsinidis and X. S. Ling, Phys. Rev. Lett. **100**, 028303 (2008)
[5] L. Laurson and M. Alava, Phys. Rev. E **74**, 066106 (2006)
[6] A. M. Troyanovski *et al.*, Nature **399**, 665 (1999)

Topological Defects in the Crystalline State of One-component Plasmas of Non-uniform Density

Adil M. Mughal[1] and M. A. Moore[2]

[1] ISI Foundation, Viale S. Severo 65 – 10133 Torino, Italy
(E-mail: adil.mughal@isi.it)
[2]The University of Manchester, School of Physics and Astronomy, Oxford Road, Manchester, England, M13 9PL
(E-mail: m.a.moore@man.ac.uk)

ABSTRACT

We study the ground state properties of classical Coulomb charges interacting with a 1/r potential moving on a plane which confined by a circular hard wall boundary. The charge density in the continuum limit is determined analytically and is non-uniform. Because of the non-uniform density there are both disclinations and dislocations present and their distribution across the system is calculated and shown to be in agreement with numerical studies of the ground state (or at least low-energy states) of N charges, where values of N up to 5000 have been studied. A consequence of these defects is that although the charges locally form into a triangular lattice structure, the lattice lines acquire a marked curvature. The scaling of various terms which contribute to the overall energy of the system of charges viz, the continuum electrostatic energy, correlation energy, surface energy (and so on) as a function of the number of particles N is determined. "Magic number" clusters are those at special values of N whose energies take them below the energy estimated from the scaling forms and are identified with charge arrangements of high symmetry.

AM would like to thank EPSRC for financial support. We would also like to thank Matthew Hastings and Paul McClarty for useful discussions.

Walls formed by Bending: Grain Boundaries and Cell Walls from Continuum Plasticity

James P. Sethna[1], SurachatfeLimkumnerd[2]

[1]James P. Sethna, Laboratory of Atomic and Solid State Physics, Cornell University, Ithaca, NY 14853-2501, USA (E-mail: sethna@lassp.cornell.edu)
[2]Physics Department,Faculty of Science, ChulalongkornUniversity, Phayathai Rd., Pathumwan,Bangkok 10330, Thailand (E-mail: surachate@sc.chula.ac.th)

ABSTRACT

In condensed-matter physics, crystals are anomalous. Most phases (liquid crystals, superfluids, superconductors, magnets, …) respond smoothly in space when strained. Crystals, when bent (an imposed rotation gradient) respond by forming sharp walls on sub-micron scales separating grains or cells. These walls are well understood microscopically, but until now science has had no simple, continuum explanation for their formation. We've discovered that these walls are explained naturally as shock fronts in a continuum theory of plasticity – analogous to the shocks formed in theories of sonic booms and traffic jams. Our theory keeps track of the topological dislocation density tensor, is derived from the microscopic dynamics using a simple closure approximation, and connects directly to engineering descriptions of strain, stress, and rotation on longer length scales. We use it to predict a new type of wall (where the dislocation-density jumps) that should form in early stages of plastic deformation.

[1] SurachateLimkumnerd and James P. Sethna,"Mesoscale theory of grains and cells: crystal plasticity and coarsening", Physical Review Letters**96**, 095503 (2006),
also written up as news article in
[2] Adrian Cho, "Theory of Shock Waves Clears Up the Puzzling Graininess of Crystals", *Science***311**, 1361 (2006).
[3]SurachateLimkumnerd and James P. Sethna,"Shocks and slip systems: Predictions from a mesoscale theory of continuum dislocation dynamics", Journal of the Mechanics and Physics of Solids (2007), doi:10.1016/j.jmps.2007.08.008.
[4]SurachateLimkumnerd and James P. Sethna, "Stress-free states of continuum dislocation fields: Rotations, grain boundaries, and the Nye dislocation density tensor", Physical Review B**75**, 224121 (2007).

This work currently supported by DOE DE-FG02-07ER45393.

A Non-Linear Multiple Slip Theory in Continuum Dislocation Dynamics

Thomas Hochrainer[1,2], **Peter Gumbsch**[1,2], **Michael Zaiser**[3]

[1]**Fraunhofer-Institut für Werkstoffmechanik IWM, Wöhlerstr. 11, 79108 Freiburg, Germany, thomas.hochrainer@iwm.fraunhofer.de;**
[2]**Institut für die Zuverlässigkeit von Bauteilen und Systemen, Kaiserstr. 12, Universität Karlsruhe, 76131 Karlsruhe, Germany, peter.gumbsch@izbs.uka.de;**
[3]**Centre for Materials Science and Engineering,The University of Edinburgh, King's Buildings, Sanderson Building, Edinburgh EH93JL, United Kingdom, m.zasier@ed.ac.uk**

ABSTRACT

Crystal plasticity is the result of the motion and complex and effectively non-linear interactions of dislocations. The collective behavior of dislocations plays a prominent role both for the evolution of dislocation structures and as origin of strain hardening. There is, however, still a major gap between microscopic and mesoscopic simulations and continuum crystal plasticity models. Only recently a higher dimensional dislocation density tensor was defined which overcomes some drawbacks of earlier dislocation density measures. The evolution equation for this tensor can be considered as a continuum version of dislocation dynamics. We use this tensor to develop a non-linear theory of multiple slip deformation. Starting from the rate of dislocation cutting events per volume, we deduce the mean area swept by dislocations between cutting events and the closely related mean free segment length. If the mean dislocation velocity depends on the mean free segment length this leads to an important non-linearity which we illustrate by means of a simple example.

1. Introduction

In recent years the understanding and modelling of collective dislocation behavior in crystal plasticity has made significant progress. Nevertheless, continuum modelling of fundamental issues like strain hardening or dislocation patterning remains an ongoing challenge. Current dislocation based continuum models of plasticity usually rely on phenomenological assumptions on the evolution of scalar dislocation densities in the spirit of Kocks [1]. One of the most advanced such models was introduced by Devincre [2], who developed a strain hardening model from an evolution equation for the mean free path of dislocations based on Kocks' equations. In the current work we use a higher dimensional dislocation density tensor [3] to deduce the mean free path and its evolution directly from the dislocation state without recourse to phenomenological equations. This leads us to a non-linear theory of multiple slip. A non-linear theory may be seen as a prerequisite to modelling – besides work hardening – also the emergence of non-equilibrium dislocation structures [4].

2. Continuum Dislocation Dynamics

At the heart of the continuum theory of dislocations developed by the authors [3] lies the so called dislocation density tensor of second order (SODT) α^{II}. This tensor is a natural generalization of the classical dislocation density tensor to a higher dimensional configuration space. It is closely related to the phase space densities of dislocations as introduced by El-Azab [5].

If dislocations move by glide only, the SODT is defined on the configuration space $Q = M \times \bigcup_\beta S^1_\beta$, where M denotes the (spatial) crystal manifold, β indicates the slip systems and the S^1_β are unit circles of directions in the respective glide planes. A point in Q is considered as composed of a spatial point p and the angle φ_β between a direction in the glide plane and the Burgers vector b_β. We may consider the SODT as a sum of tensors defined for each slip system, i.e. $\alpha^{\mathrm{II}} = \sum_\beta \alpha^{\mathrm{II}}_\beta$. On each slip system, the SODT is defined by a density function $\rho_\beta(p, \varphi_\beta)$ giving the average number (per unit area) of dislocations at p with line direction $l_\beta(\varphi_\beta)$, and a curvature function $k_\beta(p, \varphi_\beta)$ characterizing the average curvature of these dislocations. The functions ρ_β and k_β are connected by the requirement that α^{II} needs to be free of divergence in the configuration space. Although the curvature k_β does not appear explicitly in the remainder of this paper, we emphasize that its consideration is indispensable to describe the evolution of the dislocation system [3].

3. From the Rate of Dislocation Cutting to Non-linear Multiple Slip

To discuss the rate of dislocation cutting we only consider two slip systems, β and β'. Both systems may be active and the dislocations move with average velocities v_β and $v_{\beta'}$, respectively. We then find the total rate of dislocation cutting events per volume as

$$\dot{\Gamma}_{\beta\beta'} = \int_{l_\beta} \int_{l_{\beta'}} \rho_\beta\left(l_\beta\right) \rho_{\beta'}\left(l_{\beta'}\right) \left|\det\left(l_\beta, l_{\beta'}, v_\beta(l_\beta) - v_{\beta'}(l_{\beta'})\right)\right| dl_{\beta'} dl_\beta =: \int_{l_\beta} \dot{\Gamma}_{\beta\beta'}\left(l_\beta\right) dl_\beta . \quad (1)$$

A derivation of this equation will be given elsewhere. Note that we implicitly assumed the dislocations on different slip systems to be uncorrelated. More generally, the product of the two densities in the integral would be a pair density function $\rho_{\beta\beta'}\left(l_\beta, l_{\beta'}\right)$.

On the right hand side of Eqn. (1) we implicitly defined the direction-dependent rate of dislocation cutting events $\dot{\Gamma}_{\beta\beta'}\left(l_\beta\right)$. From this we evaluate the mean free area swept by dislocations between cutting events. For dislocations on glide system β with line direction l_β we find

$$A_{\beta\beta'}\left(l_\beta\right) = \frac{\rho_\beta\left(l_\beta\right) \left\| v_\beta(l_\beta) \right\|}{\dot{\Gamma}_{\beta\beta'}\left(l_\beta\right)} . \quad (2)$$

We regard the mean free area swept by a dislocation as the most natural measure for connecting plastic rates with dislocation microstructure evolution. More commonly one uses in this respect

either the mean obstacle spacing $d_{\beta\beta'}$ or the mean free path $\lambda_{\beta\beta'}$. Both are comprised in the mean free area which may be defined as $A_{\beta\beta'} = d_{\beta\beta'}\lambda_{\beta\beta'}$.

We assume conservative glide and overdamped dislocation motion, i.e. the velocity is considered proportional to the resolved shear stress τ_β in the slip system. Furthermore we make an Orowan ansatz for the friction stress $\tau^{\mathrm{f}}_{\beta\beta'}$ induced by the forest dislocations as $\tau^{\mathrm{f}}_{\beta\beta'} = a_{\beta\beta'}Gb_\beta/\sqrt{A_{\beta\beta'}}$, with the shear modulus G , and a non-dimensional constant $a_{\beta\beta'}$. The effective shear stress is defined by subtracting the friction stress from the local stress. Hence, the dislocation velocity is

$$v_\beta(l_\beta) = m|b_\beta|\,\mathrm{sign}(\tau_\beta)\left\lfloor|\tau_\beta| - a_{\beta\beta'}Gb_\beta/\sqrt{A_{\beta\beta'}(l_\beta)}\right\rfloor, \tag{3}$$

with a dislocation mobility m, the modulus of the Burgers vector $|b_\beta|$ and the square brackets acting as $\lfloor x\rfloor = 1/2\,(x+|x|)$. Obviously, this dislocation velocity in general becomes a non-linear quantity, because it contains the mean free surface $A_{\beta\beta'}$ which itself may depend on the velocity v_β.

4. Results

To illustrate possible consequences of the non-linearity contained in the above theory we assume a strongly simplified distribution of straight dislocations in a fcc crystal. Slip system β is taken as $(111)[\bar{1}10]$ while β' is $(11\bar{1})[011]$. We consider on β a homogeneous distribution of straight screw dislocations with line directions $\pm[\bar{1}10]$ and on system β' a homogeneous distribution of straight mixed dislocations with line directions $\pm[112]$ (each without excess dislocations and with equal density on both systems). These families are orthogonal to each other. The direction of motion of the dislocations on β is $\pm[\bar{1}\bar{1}2]$, while for the dislocations on β' it is $\pm[\bar{1}10]$. That is, dislocations on β move perpendicular to both the dislocation lines and the direction of motion of the dislocations on β', while the dislocations on β' move parallel to the line direction of the β dislocations. From Eqns. (1)–(3) we then find that the velocity v_β does not depend on the motion of the dislocations on β' and hence is linear in stress after exceeding the friction stress. By contrast, $v_{\beta'}$ becomes a non-linear function of stress as it depends on the velocities on both systems. We introduce dimensionless variables labelled with an underscore by dividing velocities by $m|b_\beta|\tau^{\mathrm{f}}_{\beta\beta'}$ and stresses by $\tau^{\mathrm{f}}_{\beta\beta'}$. For several velocities $\underline{v}_\beta$ the velocity $\underline{v}_{\beta'}$ is depicted in Fig.1 as a function of the dimensionless applied shear stress $\underline{\tau}'_\beta$.

The velocity $\underline{v}_{\beta'}$ shows a jump to a non-zero velocity at a critical stress depending on $\underline{v}_\beta$ and approaches linear behavior for high stresses. This implies that slip on the β system inhibits dislocation motion on the slip system β' (but not vice versa!), leading to some interesting scenarios and instabilities of the flow process associated with non-Schmid behavior: (i) initial activity on β can be stabilized beyond the point where the resolved shear stress in β' exceeds the one in β – this kinematic effect adds to the 'conventional' latent hardening; (ii) symmetrical slip on both systems

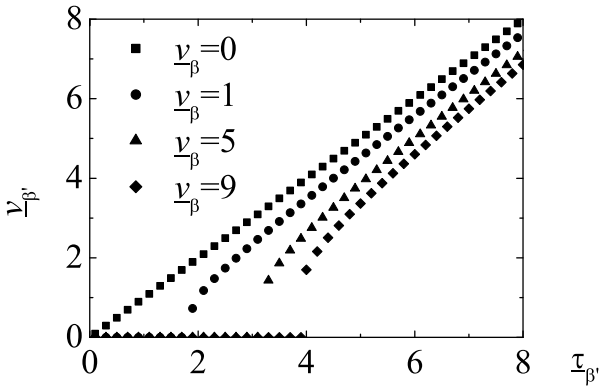

Figure 1: Stress dependence of $v_{\beta'}$ obtained from Eqns. (1)–(3) at a different velocities v_β.

is unstable as activity on β will render β' inactive; (iii) if β' is initially active, slip activity may suddenly switch to β when the resolved shear stress exceeds the critical value for the β system.

5. Summary and Discussion

We sketched a non-linear theory of multiple slip based on a higher dimensional dislocation density measure. The non-linearity was illustrated for a distribution of straight dislocations moving on two different slip systems and has been shown to produce interesting instabilities. Our simplistic example may over emphasize the non-linearity, and it remains to be seen to which extent the effects persist if more realistic dislocation distributions are assumed. In fact, a weaker non-linearity seems to be preferable, as dislocation structures only develop in later stages of deformation and strain hardening seems to be rather insensitive to details of the dislocation structure.

References

[1] U. F. Kocks, "Laws for Work-Hardening and Low-Temperature Creep", Journal of Engineering Materials and Technology, Trans. ASME, **98**, 76 (1976).

[2] B. Devincre, T. Hoc and L. Kubin, "Dislocation Mean Free Paths and Strain Hardening of Crystals", Science, **320**, 1745 (2008).

[3] T. Hochrainer, M. Zaiser and P. Gumbsch, "A Three-Dimensional Continuum Theory of Dislocations: Kinematics and Mean Field Formulation", Philosophical Magazine, **87**, 1261 (2007).

[4] G. Ananthakrishna, "Current Theoretical Approaches to Collective Behavior of Dislocations", Physics Reports, **440**, 113 (2007).

[5] A. El-Azab, "Statistical Mechanics Treatment of the Evolution of Dislocation Distributions in Single Crystals", Physical Review B, **61**, 11956 (2000).

Theoretical and Computational Modeling of the Statistics of Internal Elastic Fields in 3D Dislocation Systems

Jie Deng[1] and Anter El-Azab[2]

[1]Mechanical Engineering Department, Florida State University, Tallahassee, FL 32310
[2]School of Computational Science, Florida State University, Tallahassee, FL 32306

ABSTRACT

The statistics of internal elastic fields of 3D dislocation systems is described by probability density and pair correlation functions. Numerical results of these statistical measures are obtained for typical dislocation configurations obtained by dislocation dynamics simulation.

1. Introduction

The deformation of crystals is controlled by the collective behavior of dislocations, which has been recently described using the concepts of statistical mechanics [1-3]. In the relevant models, the evolution of dislocation density is dictated by the distribution of internal stress field [4-6]. As a result, it is important to understand the statistical properties of stress in dislocated crystals. Here, we present a statistical description of the internal stress in terms of probability density and pair correlation measures. We also generate numerical results of these measures for dislocation configurations obtained by the method of dislocation dynamics simulation [7].

2. Theoretical and Numerical Analysis

The internal stress field σ of a given dislocation configuration in a crystal volume can be divided into two contributions. The first contribution is associated with the given dislocation configuration assumed to be in an infinite-medium, σ^{∞}, and the second is called the image stress, σ^{img}. The latter either arises due to the crystal boundary or it represents the stress field generated inside the given crystal volume of interest by dislocations outside of that volume. The stress σ^{∞} is calculated using the famous line integral form for the dislocation stress in an infinite domain [8]. The stress σ^{img} is the solution of the following boundary value problem:

$$\nabla \cdot \sigma^{img}(r) + \nabla \cdot \sigma^{\infty}(r) = 0, \quad \text{with the boundary condition:} \quad \sigma^{img}(r)n(r) = -\sigma^{\infty}(r)n(r), \tag{1}$$

where $n(r)$ is the outward unit normal to the boundary. Because of the statistical nature of the dislocation distribution inside the crystal, the internal dislocation stress field σ has a statistical character. The formal connection between the internal field statistics and the dislocation

statistics can be described in terms of the probability density function (PDF) of the dislocation density. The *n*-th order PDF of the dislocation density $f^{(\alpha_1,\cdots,\alpha_n)}$ is defined such that

$$\sum_{\alpha_1,\cdots,\alpha_n}\int_{\Omega} f^{(\alpha_1,\cdots,\alpha_n)}(r_1,\theta_1,\cdots,r_n,\theta_n)dr_1 d\theta_1\cdots dr_n d\theta_n = 1. \tag{2}$$

In the above, Ω is the phase space, and r_i and θ_i are, respectively, the position and orientation of *i*-th differential dislocation segment on α_i-th slip system. Formally, the PDF p_{ij} of the internal stress tensor is expressed by

$$p_{ij}(\sigma_\circ, r) = \sum_{\alpha_1,\cdots,\alpha_n}\int_{\Omega} f^{(\alpha_1,\cdots,\alpha_n)}(r_1,\theta_1,\cdots,r_n,\theta_n)\,\delta[\sigma_\circ - \sigma_{ij}(r)]dr_1 d\theta_1\cdots dr_n d\theta_n, \tag{3}$$

where $\sigma_{ij}(r) = \sigma_{ij}(r, r_1, \theta_1, \cdots r_n, \theta_n)$ is the stress at point *r* generated by the *n* dislocation segments and $p_{ij}(\sigma_\circ, r)d\sigma_\circ$ gives the probability to find σ_{ij} falling in the range $[\sigma_\circ, \sigma_\circ + d\sigma_\circ]$ at point *r*. With periodic boundary conditions applied in the dislocation dynamics simulation, the distribution of dislocation density and associated internal fields is translation invariant. In this case, the PDF for stress simplifies to

$$p_{ij}(\sigma_\circ) = \int_V p_{ij}(\sigma_\circ, r)\Big/V, \tag{4}$$

where *V* is the simulation volume and $p_{ij}(\sigma_\circ)d\sigma_\circ$ gives the probability to find σ_{ij} falling in the range $[\sigma_\circ, \sigma_\circ + d\sigma_\circ]$ at a random point. While $p_{ij}(\sigma_\circ)$ provides the distribution of single stress, the inter-dependence between stress values at two distinct points is described in terms of the pair correlation

$$C_{ijkl}(\Delta r) = \left\langle \sigma_{ij}(r)\sigma_{kl}(r+\Delta r)\right\rangle \Big/ \sqrt{\left\langle \sigma_{ij}^2(r)\right\rangle\left\langle \sigma_{kl}^2(r+\Delta r)\right\rangle}, \tag{5}$$

where $<\cdot>$ denotes the ensemble average—it is equivalent to the volume average here due to the translation invariance. We thus have $\left\langle \sigma_{ij}(r)\right\rangle = \left\langle \sigma_{kl}(r+\Delta r)\right\rangle = 0$. The positive (respectively negative) values of $C_{ijkl}(\Delta r)$ implies that the stress values at two points separated by Δr have the same (respectively opposite) signs.

The ParaDiS dislocation dynamics code [7] has been used to obtain the dislocation configuration required for computing internal fields in a BCC crystal loaded in [100] direction. The simulation box is a cube of edge *L* close to 5 microns, which is divided into $30\times30\times30$ volume elements for the purpose of computing the internal stress using the finite element method. In computing the PDF and pair correlation functions for the stress field, the stress value at the center of each volume element is considered and the range of Δr in the pair correlations is confined to [*-0.75L,0.75L*] to avoid the edge effect.

Figure 1 shows the probability distribution of six stress components for typical dislocation configurations generated by ParaDiS code at strains of ε=0.0012 and ε=0.015 and strain rate $\dot{\varepsilon}$=1/s. It has been found that the distribution of stress components is nearly Gaussian, with zero mean value and variances that depend on the strain. The zero mean value is consistent with the self-balanced nature of internal stress, and the dependence of variance on strain is due to the increase of dislocation density—at high dislocation density, the probability of finding larger stress values at a random point is higher. It has also been found that the normal (diagonal) stress components have large variances than the shear stresses.

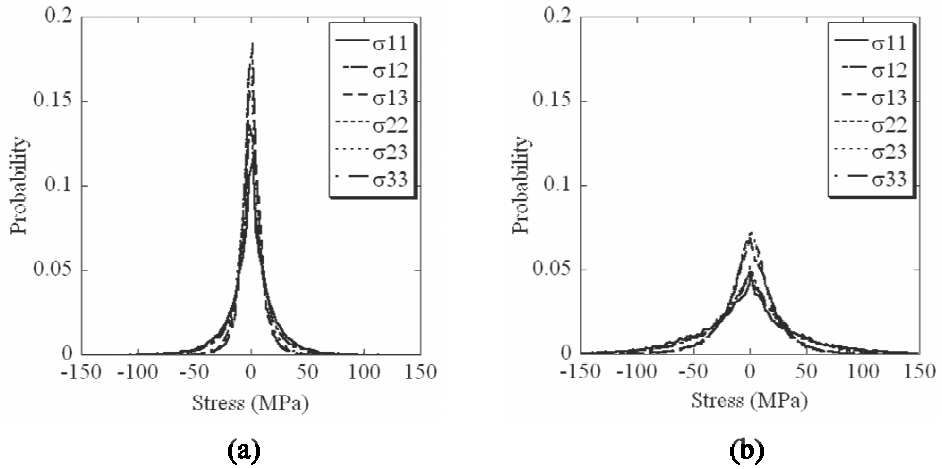

Figure 1. Sample result for the probability distribution of internal stress of a complex dislocation configuration.

Figure 2 shows a sample pair correlation result for the stress component σ_{23} at ε=0.005 (a and b) and σ_{33} at ε=0.0096 (c and d). The correlation is displayed over the Δx-Δy plane in parts a and c, and over the Δx-Δz plane in b and d. The strain rate was $\dot{\varepsilon}$=10/s. The pair correlation exhibits multiple secondary peaks distributed anisotropically in space. These positive correlation peaks indicate that the stress mode (tension or compression) at two points are the same. The anisotropic nature and the correlation fluctuations in space (and associated wavelengths) are similar to the corresponding characteristics of the dislocation density correlation, indicating that the natural connection between the distribution of internal stress and the distribution of underlying dislocation structure.

3. Summary

A theoretical and computational approach for calculating the internal elastic fields of dislocations and their statistics has been outlined. The probability density function and pair correlation of internal fields are modeled in terms of generalized dislocation density distribution function. The numerical simulation of those statistical models is implemented for dislocation configurations obtained from dislocation dynamics simulation. The spatial distribution of internal dislocation

stress, which is illustrated by the PDF and pair correlations, provides a great deal of insight into the origin of formation of various dislocation patterns in deformed crystals. Work is underway to incorporate the internal stress fluctuations with the dislocation density fluctuations and exploit this connection to complete the statistical description of dislocation and mesoscale theory of crystal plasticity.

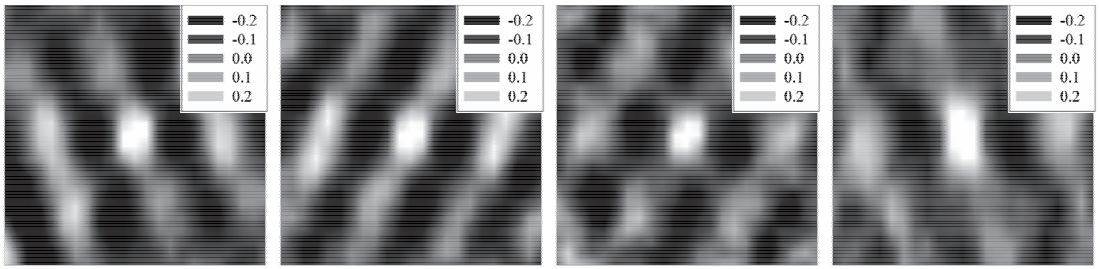

Figure 2. Pair correlations of internal stress field for the similar dislocation configuration considered in figure 1 above.

Acknowledgements

This work was supported by the Office of Basic Energy Sciences of the U.S. Department of Energy, through contract number DE-FG02-08ER46494 at Florida State University.

References

[1] I. Groma, "Link between the microscopic and mesoscopic length-scale description of the collective behavior of dislocations," Physical Review B **56**, 5807 (1997).
[2] M. Zaiser, "Statistical modeling of dislocation systems," Materials Science and Engineering A, **309-310**, 304 (2001).
[3] A. El-Azab, "Statistical mechanics treatment of evolution of dislocation distribution in single crystals," Physical Review B **61**, 11956 (2000).
[4] I. Groma and B. Bako, "Probability distribution of internal stresses in parallel straight dislocation systems," Physical Review B, **63**, 224012 (1998)
[5] F. Csikor and I. Groma, "Probability distribution of internal stress in relaxed dislocation systems," Physical Review B, **70**, 064106 (2004)
[6] M. Zaiser and A. Seeger, "Long-range internal stresses, dislocation patterning and work-hardening in crystal plasticity," in Dislocation in Solids, edited by F. R. Nabarro (Elsevier Science, Amsterdam 2002) Vol 11, 1-101
[7] A. Arsenlis, W. Cai, M. Tang, et al., "Enabling strain hardening simulations with dislocation dynamics," Modeling and Simulation in Materials Science and Engineering, **15**, 553 (2007).
[8] J. Hirth and J. Lothe, Theory of Dislocations (John Wiley & Sons, New York 1982).

3D Dislocation Pair Correlation Functions from DDD Simulations

Ferenc F. Csikor[1], István Groma[1], Thomas Hochrainer[2], Daniel Weygand[3], Michael Zaiser[4]

[1]Department of Materials Physics, Eötvös University Budapest, Pázmány Péter sétány 1/a, H-1117 Budapest, Hungary (csikor@metal.elte.hu, groma@metal.elte.hu)
[2]Fraunhofer-Institut für Werkstoffmechanik IWM, Wöhlerstr. 11., 79108 Freiburg, Germany (thomas.hochrainer@iwm.fhg.de)
[3]Institut für Zuverlässigkeit von Bauteilen und Systemen (izbs), University of Karlsruhe, Kaiserstr. 12., 76131 Karlsruhe, Germany (daniel.weygand@izbs.uni-karlsruhe.de)
[4]Centre for Materials Science and Engineering, University of Edinburgh, King's Buildings, Sanderson Building, Edinburgh EH9 3JL, UK (M.Zaiser@ed.ac.uk)

ABSTRACT

Statistical mechanics studies of 2D systems of straight, parallel dislocations have led Groma et al. to a physically sound prototype continuum theory for bridging the micro- and mesoscales of crystal plasticity. Groma's theory takes the form of a hierarchy of interconnected evolution equations for different order dislocation densities which needs to be cut at a certain level to arrive at a closed theory. It has been clearly demonstrated [1] that cutting the hierarchy at first order and utilizing the pair correlation functions of homogeneous dislocation systems leads to a theory capable to describe all ensemble averaged physical quantities observed in 2D discrete dislocation dynamics (DDD) simulations. The numerical finding that 2D dislocation pair correlations are short ranged is decisive for the theory as this is what enables a local theory.
The authors of the present paper are involved in generalizing Groma's theory to the 3D dislocation problem by studying the statistical mechanics of curved dislocation lines [2]. In the generalized theory, the range of dislocation pair correlations is expected to play a similar decisive role as in the 2D version. The present paper discusses the analytical properties of dislocation pair correlation functions numerically calculated from a large number of 3D DDD simulations. In particular, the spatial range and history dependence of the conventional and stress weighted pair correlation functions will be detailed, continuing the work in [3]. The results will be compared to existing analogous simulations [4].

[1] I. Groma, F. F. Csikor, and M. Zaiser, "Spatial Correlations and Higher-Order Gradient Terms in a Continuum Description of Dislocation Dynamics", Acta Materialia, **51**, 1271 (2003).
[2] T. Hochrainer, M. Zaiser, and P. Gumbsch, "A Three-Dimensional Continuum Theory of Dislocation Systems: Kinematics and Mean-Field Formulation", Philosophical Magazine, **87**, 1261 (2007).
[3] F. F. Csikor, I. Groma, T. Hochrainer, D. Weygand, and M. Zaiser, "On the Range of 3D Dislocation Pair Correlations", in Proc. of the 11th International Symposium on Continuum Models and Discrete Systems, D. Jeulin et al. (eds.), Mines ParisTech, Paris, 271 (2007).
[4] J. Deng and A. El-Azab, "Dislocation Pair Correlations from Dislocation Dynamics Simulations", Journal of Computer-Aided Materials Design, **14**, 295 (2007).

Intermittent Crack Growth in Heterogeneous Brittle Materials

Daniel Bonamy[1], Stéphane Santucci[2], Laurent Ponson[1,4], Knut-Jorgen Maloy[2]

[1]CEA, IRAMIS, SPCSI, Grp. Complex Systems & Fracture, F-91191 Gif sur Yvette Cedex, France;
[2]Fysisk Institutt, Universitetet Oslo, P.O. Boks 1048 Blindern, N-0316 Oslo 3 Norway;
[3]Division of Engineering and Applied Science, California Institute of Technology, Pasadena, CA 91125, USA.
(E-mail : daniel.bonamy@cea.fr)

ABSTRACT

The effect of materials heterogeneities onto their failure properties remains far from being understood. In particular, in heterogeneous materials under slow external loading, cracks growth often displays a jerky dynamics, with sudden jumps spanning over a broad range of length-scales, as also suggested from the acoustic emission accompanying the failure of various materials and - at much larger scale - the seismic activity associated to earthquakes. Presently, this intermittent "crackling" dynamics cannot be captured by standard Linear Elastic Fracture Mechanics (LEFM).
In this presentation, we will see how to extend LEFM to derive a stochastic description of slow crack growth in heterogeneous media [1]. This description succeeds in reproducing the crackling dynamics classically observed. Its predictions will then be confronted to experimental observations performed at University of Oslo on the 2D crack propagation within a transparent Plexiglas block [2]. All the statistical features are perfectly reproduced. In this description, slow crack growth in inhomogeneous media appears as a self-organized critical phase transition. As such, it exhibits universal – and, to some extent, predictable – features insensitive to the materials nature and the loading conditions. In this respect, we argue that this linear elastic stochastic description contains all the ingredients needed to capture the crack dynamics in a broad range of situations, from nanostructured materials to earthquakes. Finally, we will discuss – and confront to experiments – some predictions of this stochastic LEFM description onto the morphology of fracture surfaces [3].

[1] D. Bonamy, S. Santucci and L. Ponson, Physical Review Letters **101**, 045501 (2008).
[2] K.-J. Maloy, S. Santucci,, J. Schmittbuhl and R. Toussaint, Physical Review Letters **96**, 045501 (2006).

Daniel Bonamy acknowledges funding from French ANR through grant No. ANR-05-JCJC-0088. Stéphane Santucci was supported by the NFR Petromax Program No. 163472/S30..

Analysis of Fracture Roughness using 2D Beam Lattice Systems

Phani K. Nukala[1], Stefano Zapperi[2], Mikko J. Alava[3], Srdjan Simunovic[4]

[1]Computer Science and Mathematics Division, Oak Ridge National Laboratory, Oak Ridge, TN 37831-6164 (E-mail: nukalapk@ornl.gov)
[2]INFM-CNR, S3, Dipartimento di Fisica, Universita di Modena e Reggio Emilia, I-41100, Modena, Italy (E-mail: stefano.zapperi@unimore.it)
[3]Laboratory of Physics, Helsinki University of Technology, FIN-02015, HUT, Finland, (E-mail: mjalava@cc.hut.fi)
[4]Computer Science and Mathematics Division, Oak Ridge National Laboratory, Oak Ridge, TN 37831-6164 (E-mail: simunovics@ornl.gov)

ABSTRACT

We investigate whether anomalous scaling of crack roughness as observed in fuse lattice models is a generic feature of two-dimensional crack profiles obtained using discrete lattice models. For this purpose, we study the scaling of crack roughness using large scale 2D and 3D beam lattice systems. In 2D, our results indicate that the crack roughness obtained using beam lattice systems does not exhibit anomalous scaling in sharp contrast to the simulation results obtained using fuse lattice systems. That is, the local and global roughness exponents (ζ_{loc} and ζ, respectively) are equal to each other, and the two-dimensional crack roughness exponent is estimated to be $\zeta_{loc} = \zeta = 0.64$ +/- 0.02. The origin of anomalous scaling in fuse lattice systems appears to be due to scalar nature of fuse systems (anti-planar shear model), which readily allows for crack branching. We verified this with a simplified crack branching beam model, which indeed exhibits anomalous scaling of crack roughness. Removal of overhangs (jumps) in the crack profiles however only partially suppresses this anomalous scaling. Furthermore, removing jumps in the crack profile completely eliminates the multi-scaling observed in earlier studies. We also find that the probability density distribution $p(\Delta h(l))$ of the height differences $\Delta h(l) = [h(x+l) - h(x)]$ of the crack profile obtained after removing the jumps in the profiles follows a Gaussian distribution even for small window sizes (l). Analysis of roughness of fracture surfaces using 3D beam lattice systems is currently underway and will be discussed during the presentation.

This research is sponsored by the Mathematical, Information and Computational Sciences Division, Office of Advanced Scientific Computing Research, U.S. Department of Energy under contract number DE-AC05-00OR22725 with UT-Battelle, LLC. MJA and SZ gratefully thank the financial support of the European Commissions NEST Pathfinder programme TRIGS under contract NEST-2005-PATH-COM-043386. MJA also acknowledges the financial support from The Center of Excellence program of the Academy of Finland.

Shear failure of thin films on disordered substrates: Nucleation and propagation of interfacial shear cracks.

M. Zaiser[1], P. Moretti[1,2], A. Konstantinidis[3], E.C. Aifantis[3,4]

[1]The University of Edinburgh, Center for Materials Science and Engineering, The King's Buildings, Sanderson Building, Edinburgh EH93JL, UK (M. Zaiser@ed.ac.uk)
[2]Departament de Fisica Fonamental, Facultat de Fisica, Universitat de Barcelona, Marti i Franques 1, E-08028 Barcelona, Spain (paolo.moretti@ub.edu)
[3]Laboratory of Mechanics and Materials, Aristotle University of Thessaloniki, 54124 Thessaloniki, Greece (akonsta@gen.auth.gr)
[4]Center for the Mechanics of Material Instabilities and Manufacturing Processes (MMIMP), Michigan Tech., Houghton, USA (mom@mom.gen.auth.gr)

ABSTRACT

We formulate a theoretical model of the shear failure of a thin film tethered to a rigid substrate. The interface between thin film and substrate is modeled as a cohesive layer with randomly fluctuating strength/fracture energy. We demonstrate that, on scales large compared with the film thickness, the internal shear stresses acting on the interface can be approximated by a second-order gradient of the shear displacement across the interface. The model is used to study one-dimensional shear cracks, for which we evaluate the stress-dependent probability of nucleation of a critical crack and the concomitant disorder dependence of interfacial shear strength.

1. Introduction

In this study we investigate the interfacial failure of thin films subject to shear loads. We consider films where the interface with the substrate is disordered, such that the interfacial shear strength as well as the fracture energy are random functions of position. While most of the mechanics literature has focused on the properties of interface cracks in systems where the properties of the interface are spatially homogenous, failure of disordered interfaces with randomly fluctuating strength has been investigated in a number of papers in statistical physics journals [1-4]. Besides obvious applications to materials problems such as shear failure of coatings and shear-induced delamination of thin films, the problem at hand has some interesting applications in geosciences [5-7], where models similar to the one studied in this paper have been applied to the initiation of snow avalanches and landslides.

In the present study we investigate theoretically how random variations of interface toughness affect the nucleation of interface cracks. We assume a one-dimensional geometry and evaluate the crack nucleation probability as a function of stress, geometry, and the statistical parameters characterizing the interfacial strength distribution. The theoretical arguments are validated by comparison with numerical simulations.

2. Formulation of the model

We consider a thin elastic film tethered to a rigid substrate. The film is loaded in plane shear. The interface is modeled as a cohesive layer at z=0, which is characterized by a scalar stress-displacement relationship $\sigma_{xy}(x, z=0) = \tau(u)$ where σ_{xy} is the shear stress in the film, τ is the interfacial shear strength, and $u(x) = w_x(x, z=0)$ is the displacement across the interface. The maximum stress that can be supported by the interface is denoted as τ_M, and the failure energy is given by the integral

$$w_f = \int \tau(u)\mathrm{d}u =: \tau_M u_0 \,, \tag{1}$$

where u_0 denotes the characteristic displacement-to-failure. Stress-displacement relationships are schematically shown in Fig. 1 for the semi-brittle (full line) and brittle cases (dashed line).

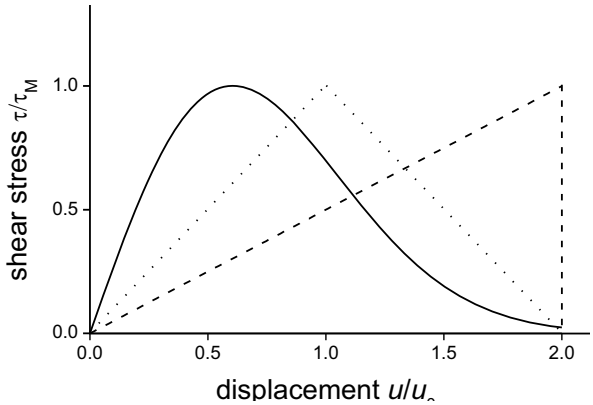

Figure 1. Shear strength versus interfacial displacement (schematically); full line: semi-brittle behaviour, dashed line: brittle behaviour; dotted line: piecewise linear approximation to the semi-brittle case as used in our simulations.

Structural disorder is introduced into the model in terms of statistical variations of τ_M which is considered a stochastic process with prescribed statistical properties.

To analyze crack nucleation and propagation, we have to evaluate the internal stresses associated with the interfacial displacement field $u(x)$. The elastic energy functional associated with a generic displacement vector field $\mathbf{w}(\mathbf{r})$ is given by

$$H(\mathbf{w}) = \frac{\mu}{2}\int \left[\alpha(\mathrm{div}\mathbf{w})^2 + (\mathrm{curl}\mathbf{w})^2\right]\mathrm{d}^3 r \,, \tag{2}$$

where $\alpha = (2-2\nu)/(1-2\nu)$, and ν is Poisson's number. Energy minimization gives the equilibrium equation

$$\nabla^2\mathbf{w} + \frac{1}{1-2\nu}\,\mathrm{grad}\left(\mathrm{div}\,\mathbf{w}\right) = 0\,. \tag{3}$$

We solve Eqn. 3 in Fourier space, imposing along the z=0 plane the boundary condition $w_x(x, z=0) = u(x)$, $w_y = w_z = 0$ and making the crucial assumption that the film thickness D is much smaller than the characteristic length of variations in the displacement field: $|\mathbf{k}D| << 1$ where $\mathbf{k}$ is the wave vector. The elastic energy can then be written as

$$H(u) = \frac{1+\alpha}{2} D\mu \int \left(\frac{\partial u}{\partial x} \right)^2 \mathrm{d}x \tag{4}$$

The total energy of the system is obtained by adding to the elastic energy H the work done by the shear stresses at the interface:

$$G(u) = -\int \mathrm{d}x \left[\int_0^{u(x)} \left(\sigma_{xy}^{\mathrm{EXT}} - \tau(u) \right) \mathrm{d}u \right], \tag{5}$$

Minimization of the total energy functional $E(u) = G(u) + H(u)$ leads to the equilibrium condition

$$I \frac{\partial^2 u}{\partial x^2} + \sigma_{xy}^{\mathrm{EXT}} - \tau(u) \le 0, \tag{6}$$

where the gradient coefficient is given by $I = 2D\mu(1+\alpha)$. Equations of this type have been studied by Aifantis and co-workers in the context of shear and slip bands in metal plasticity (see e.g. [8]). It may be noted that in these cases the constitutive relation (Eqn. 6) contains a strain variable (shear strain or equivalent strain) in place of the displacement variable u. The mathematical structure is, however, the same as in the present problem.

3. Energy of a shear crack and critical crack size

We first consider interfaces with space independent fracture toughness. A mode-II crack is assumed to exist along the interface. Such a crack is characterized by a displacement field which, for $x \to -\infty$, starts from a value u_0 on the left stable branch of the $\tau(u)$ curve, goes through a maximum u_1 which without loss of generality we assume at $x=0$, and then reverts to u_0 for $x \to \infty$. The derivation of the corresponding solutions of Eqn. 6 has been discussed elsewhere [7]. In the limit of long cracks (small stresses) we find that the displacement profile is approximately parabolic,

$$u(x) = \frac{\left(l^2 - x^2 \right) \sigma_{xy}^{\mathrm{EXT}}}{2I}, \tag{7}$$

where the parameter l can be interpreted as the crack length. This equation describes the displacement profile as long as $u >> u_0$, such that $\tau(u) \sim 0$. The parabolic profile is complemented by two boundary layers where the shear strength $\tau(u)$ goes through the curve depicted in Figure 1. For a long crack the contribution of these boundary layers to the total energy can be neglected, and the energy is approximately given by

$$E(l) \approx -\frac{l^3}{3I} \left(\sigma_{xy}^{\mathrm{EXT}} \right)^2 + 2 w_f l \quad . \tag{8}$$

This energy has a saddle point at the critical crack length $l_c = \sqrt{2 w_f I} \Big/ \sigma_{xy}^{\mathrm{EXT}}$. Cracks above this length are unstable under the corresponding load and lead to interface failure. The energy required to create a critical crack is $E_c = 4 w_f l_c / 3$. We now proceed to analyse the question under which conditions crack nucleation can occur spontaneously in a disordered medium.

4. Shear crack nucleation at a disordered interface

A disordered interface can be described by a randomly varying peak shear strength $\tau_M(x)$ or, equivalently, failure energy $w_f(x)$. In this case, the energy expression, Eqn. 8, modifies to

$$E(l) \approx -\frac{l^3}{3I}\left(\sigma_{xy}^{\mathrm{EXT}}\right)^2 + \int_{-l}^{l} w_f(x)\mathrm{d}x = \int_{-l}^{l}\left[w_f(x) - F(x)\right]\mathrm{d}x \quad , \tag{9}$$

where $F(x) = \left(x\sigma_{xy}^{\mathrm{EXT}}\right)^2/(2I)$ is the effective driving force acting on the edge of a crack of length x.

A sufficient criterion for spontaneous nucleation of a propagating shear crack (starting from the position x=0) is given by $(\partial E/\partial l) < 0\ \forall l$ or, equivalently, by $F(l) > w_f(l)\ \forall l$. To estimate the probability for this to happen, we assume that the failure energy variations can be characterized by a finite correlation length ξ. We split the interface into segments of length ξ and treat the shear strengths in each segment as independent, identically distributed random variables with probability distribution $P(w_f)$. The condition that the crack can advance across the nth segment is $F(n\xi) > w_f(n\xi)$, the probability for this is $P(F(n\xi))$, and the crack nucleation probability is $W_{\mathrm{nucl}} = \prod_n P(F(n\xi))$. Taking the logarithm and reverting to continuous variables, we obtain

$$\ln W_{\mathrm{nucl}} = \frac{1}{\xi}\int \ln P(F(x))\mathrm{d}x \ . \tag{10}$$

To evaluate this probability we have to specify the probability distribution characterizing the variations of interfacial strength. We assume a Weibull distribution with characteristic failure energy w_0 and modulus β:

$$P(w_f) = 1 - \exp\left[-\left(\frac{w_f}{w_0}\right)^{\beta}\right] \tag{11}$$

Using the driving force given above, the crack nucleation probability is then evaluated as

$$\ln W_{\mathrm{nucl}} = \frac{1}{\xi}\int \ln P(F(x))\mathrm{d}x = \frac{\sqrt{2Iw_0}}{\xi\sigma_{xy}^{\mathrm{EXT}}}\int \ln[1-\exp(-s^{2\beta})]ds = -\frac{\sqrt{2Iw_0}}{\xi\sigma_{xy}^{\mathrm{EXT}}}\,g(\beta), \tag{12}$$

where s=x/l_c is the ratio between the crack size and the size of a deterministic critical crack. Hence we obtain that

$$W_{\mathrm{nucl}} = \exp\left[-g(\beta)\frac{\sqrt{2Iw_0}}{\xi\sigma_{xy}^{\mathrm{EXT}}}\right] = \exp\left[-\frac{E_C}{k_B T_{\mathrm{EFF}}}\right]. \tag{13}$$

This has the structure of an Arrhenius expression where the activation energy is the energy of a critical crack in the system without disorder and the place of temperature is taken by an effective 'disorder temperature' $k_B T_{\mathrm{eff}}$=$4\xi w_0/3g(\beta)$. For large β, we may approximate the integrand in Eqn. 12 by $\ln s^{2\beta}$ for s<1, and 0 for s>1. In physical terms, this means that only crack sizes up to the critical one significantly affect the nucleation probability, which is thus tantamount to the probability of forming a critical 'deterministic' crack. In this limit, we simply obtain that $g(\beta) = 2\beta$. With this approximation, the effective 'disorder temperature' is directly proportional to the variance of the Weibull distribution times the correlation length of the strength variations.

Nucleation of a propagating crack implies system failure. However, Eqn. 13 cannot be directly interpreted as a system failure probability: While Eqn. 13 is evaluated under the assumption that the crack starts from the origin, nucleation from any other position would produce a similar result. To evaluate the corresponding size dependent correction, we observe that only crack sizes up to the critical one affect the nucleation probability. Hence the deterministic critical crack size acts as an effective correlation length, and regions that are separated by more than this length behave in a statistically independent manner. We may therefore divide a system of length L into $N=L/l_c$ independent regions and define the stress-dependent system failure probability as the probability that, at a given stress, a crack has nucleated in the weakest region. This problem can be rigorously addressed using the methods of extreme order statistics. To obtain a simple estimate, however, one can simply assume that failure occurs at the stress where the failure probability for any given region becomes of the order of $1/N$. From this estimate and Eqn. 13, we see that the mean failure stress is expected to scale like

$$\sigma_{xy}^{\mathrm{FAIL}} = \left[2g(\beta) \frac{\sqrt{2Iw_0}}{\xi \ln N} \right] \tag{14}$$

It is interesting to compare this relationship with the deterministic failure stress of a system containing a crack of length l: $\sigma_{xy}^{\mathrm{EXT}} = \sqrt{2w_f I} \Big/ l$. It is evident that, in Eqn. 14, the correlation length of the disorder plays a very similar role to the crack size in case of a interface without disorder but containing a deterministic crack.

5. Comparison with simulation results

To test the above calculations, we use a lattice automaton technique where we evaluate the displacements at discrete sites x_i on a one-dimensional lattice with lattice constant Δx. Accordingly, we replace u_{xx} in Eqn. 6 by the corresponding discrete second-order gradient. Furthermore we approximate the strength-displacement characteristics by a piecewise linear curve as shown by the dotted line in Figure 1. Nondimensional variables are defined through

$$T = \frac{\tau}{\langle \tau_{\mathrm{M}} \rangle}, S = \frac{\sigma_{xy}^{\mathrm{EXT}}}{\langle \tau_{\mathrm{M}} \rangle} = U = \frac{u}{u_0}, X = \left(\frac{Iu_0}{\langle \tau_{\mathrm{M}} \rangle} \right)^{-1/2} \tag{15}$$

such that the average peak strength and fracture energy are by definition equal to 1. Random values for the local peak strengths are generated as Weibull distributed random fields with average 1, spatial correlation length ξ and Weibull parameter β. Note that the nondimensional values of these two statistical parameters, together with the system size, are the only independent parameters of the problem.

The system is slowly loaded by increasing the external stress S from zero in small steps until sites become unstable as the local (external plus internal) stress exceeds the local shear strength. The displacement at all unstable sites is then increased by a small amount ΔU. New internal stresses are computed for all sites and it is checked again where the sum of external and internal stresses exceeds the local strength. The displacement at the now unstable sites is further increased, and the process is repeated until the system has reached a new stable configuration. Then the external stress is increased again and so on until the system has failed completely ($U_i>2$ for all sites). The corresponding *critical stress* is recorded, and the procedure is repeated for different realizations. Figure 2 shows the results of simulations carried out for a nondimensional correlation length of 10, system size 800, and varying Weibull exponents

β. It is seen that the agreement between simulations and theoretical predictions is excellent. The deviation at large β is readily understood by observing that the failure stress for a homogeneous system without crack (the limit of infinite β) can never exceed the (average) peak strength which here is equal to 1. In the formalism, this effect can be taken into account by accounting, in the derivation of the crack properties, for a finite process zone size as discussed by Bazant [9]. A more detailed discussion of this problem, and the extension of our treatment to two dimensions, will be given elsewhere.

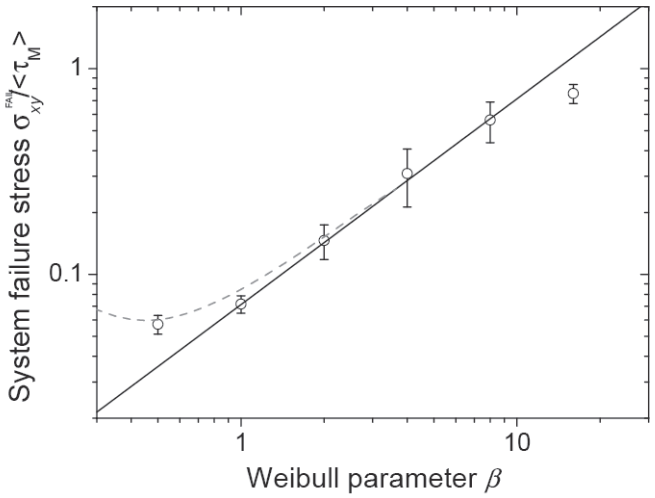

Figure 2: Comparison between calculated and simulated system failure stresses. Data points: simulation results (the error bars indicate the variance of failure stresses from 5 simulations), full line: Prediction according to Eqn. 14 with $g(\beta) = 2\beta$, dashed line: prediction with numerical evaluation of $g(\beta)$.

References

[1] M.J. Alava, P.K.N.N. Nukala, and S. Zapperi, "Statistical models of fracture". Advances in Physics **55**, 349-476 (2006).

[2] F. Raischel, F. Kun and H.J. Herrmann, "A simple beam model for the shear failure of interfaces", Phys. Rev. E, **72**, 046126 (2005).

[3] R. Cruz Hidalgo, Y. Moreno, F. Kun and H.J. Herrmann, "A fracture model with variable range of interaction", Phys. Rev. E, **65**, 046148 (2002).

[4] P.F. Arndt and T. Nattermann, "Criterion for crack formation in disordered materials", Physical Review B, **63**, 134204 (2001).

[5] M. Zaiser, "Slab Avalanche Release Viewed as Interface Fracture in a Random Medium", Ann. Glaciol., **38**, 79-83 (2004).

[6] B. Fyffe and M. Zaiser, "The effects of snow variability on slab avalanche release", Cold Reg. Sci. Techn., **40**, 229-242 (2004).

[7] B. Fyffe, M. Zaiser and E.C. Aifantis, "Shear bands and damage clusters in slope failure – a one-dimensional model", J. Mech. Beh. Mater., **15**, 185-202 (2004).

[8] H.M. Zbib and E.C. Aifantis, "On the structure and width of shear bands", Scripta Metall. Mater., **22**, 703-708 (1988).

[9] Z.P. Bazant and J. Planas, Fracture and Size Effect in Concrete and Other Quasibrittle Materials, CRC Press, Boca Raton (FLA) 1998.

Strength of Heterogeneous Materials with Flaws

Mikko Alava[1], Phani K. Nukala[2], Stefano Zapperi[3]

[1]Helsinki University of Technology, Department of Engineering Physics, PO Box 1100, HUT 02015, Finland (E-mail: Mikko.Alava@tkk.fi)
[2]Computer Science and Mathematics Division, Oak Ridge National Laboratory, Oak Ridge, TN 37831-6164, USA (E-mail: nukalapk@ornl.gov)
[3]CNR-INFM, S3, Dipartimento di Fisica, Universita di Modena e Reggio Emilia, Via G. Campi 213A, 41100 Modena, Italy and ISI Foundation, Viale S. Severo 65, 10133 Torino, Italy, (E-mail: Stefano.zapperi@unimore.it)

ABSTRACT

The theory of the strength of specimens with flaws depends on the presence of disorder and the intrinsic response of the material. Here, we analyze the fundamentals of the problem using scaling theory from statistical physics and extensive simulations of lattice models of fracture, both with scalar (random fuse model) and vectorial (spring model, beam model) interactions. We present a formula incorporating three important effects: classical Linear Elastic Fracture Mechanics for moderate-to-large flaws, the presence of a fracture process zone (FPZ), and the intrinsic scaling of the strength of the material at hand. These all, in particular the FPZ, depend fundamentally on the presence of disorder [1,2] Extensions including statistical strength distributions and the crack growth resistance (R-curve) will be discussed.

[1] M.J. Alava, P.K. Nukala, and S. Zapperi, "Role of Disorder in the Size Scaling of Material Strength", Physical Review Letters **100**, 055502, 2008).
[2] Mikko J. Alava, Phani KV.V. Nukala, and Stefano Zapperi, "Fracture Size Effects from Disordered Lattice Models", arXiv:0804.2224 (25 pages), submitted for publication to International Journal of Fracture.

Sponsored by DOE, grant DE-AC05-00OR22725 and the European Commission's NEST Pathfinder program TRIGS, contract NEST-2005-PATH-COM-043386.

Deformation in disordered solids: Correlations in displacement derivatives and avalanche distributions

Craig E. Maloney[1,2], K. Michael Salerno[1], Mark O. Robbins[1]

[1]Dept. Physics & Astronomy, Johns Hopkins University, 3400 N. Charles St., Baltimore, MD 21218 (E-mail: mr@jhu.edu)
[2]Civil and Environmental Engineering, Carnegie Mellon University, 5000 Forbes Ave., Pittsburgh, PA 15213 (E-mail: craigmaloney@cmu.edu)

ABSTRACT

Deformation of a model 2D amorphous solid is studied using molecular dynamics simulations. Correlations in displacement derivatives and the statistics of avalanches are studied as the stress increases to the peak yield stress and in steady-state shear. The solids are nearly incompressible, so the divergence of the displacement is small. Striking correlations are observed in the curl of the displacement field which quantifies both the magnitude and direction of local shear. The correlations are strongly anisotropic, with shortest range along the compressive and tensile directions, and longest range along shear directions. In steady state deformation, correlations decay as a power of wavevector. Both the prefactor and the scaling exponent vary with direction [1]. The scaling exponent has four-fold symmetry, while the prefactor has only two-fold symmetry. This can be explained by considering the Mohr-Coulomb model for plastic deformation. The displacements produced by avalanches are also strongly anisotropic and the distribution of the amount of energy dissipated in an avalanche follows a power law. The non-affine displacement of particles grows diffusively with time, but spatial correlations in successive avalanches lead to a diffusion constant that scales linearly with system size [2].

[1] C.E. Maloney and M.O. Robbins, "Long-ranged anisotropic strain correlations in sheared amorphous solids", submitted to Physical Review Letters.
[2] C.E. Maloney and M.O. Robbins, "Evolution of displacements and strains in sheared amorphous solids", Journal of Physics: Condensed Matter, **20**, 244128 (2008).

This material is based on work supported by the National Science Foundation under Grant No. DMR-0454947 and PHY-99-07949.

Colloidal Glasses Visualize Multiscale Plasticity in Amorphous Solids

Peter Schall

Van der Waals-Zeeman Institute, University of Amsterdam, Amsterdam, The Netherlands
(E-mail: p.schall@uva.nl)

ABSTRACT

Colloids are small particles of the order of a micrometer, suspended in a solvent. Because of their Brownian motion, the particles form phases (gas, liquid, glass, crystal) similar to those formed by atoms in different states of matter. Due to the much larger length- and time scales compared to atoms, colloids can be studied with optical microscopy, making them powerful models for investigating condensed matter at the "atomic" scale. We use colloidal glasses to obtain insight into the flow of amorphous materials. In three dimensions and real time, we track the individual colloidal particles in a flowing glass, and we visualize structural rearrangements that occur during flow. The individual particle trajectories are used to identify regions of non-affine deformation, in which shear concentrates. Under slow shear, we observe thermally activated 'shear transformation zones' embedded in an otherwise elastic amorphous material. Correlations between these zones, mediated through their long-range stress field, result in flow, which is homogeneous on macroscopic length scales.

Defects in Amorphous Solids

Craig E. Maloney

Civil and Environmental Engineering, Carnegie Mellon University, 5000 Forbes Ave., Pittsburgh, PA 15213 (E-mail: craigmaloney@cmu.edu)

ABSTRACT

The identification of the most elementary underlying defects in a material is crucial to constructing models which describe the behavior at coarser scales. In crystal plasticity, there is universal agreement that these defects consist of dislocations in the crystal. In the plastic response of amorphous systems, the situation is not so clear. One emerging point of view is that the plasticity in these system is governed by a class of local defects known as shear transformation zones. We will discuss various issues related to the identification, characterization, and organization of these defects utilizing molecular dynamics simulations and statistical analysis of heterogeneity in the local mechanical response of model systems.

Dynamics of Cracking Noise during Peeling of an Adhesive Tape

Jagadish Kumar [1], M. Ciccotti [2] and G. Ananthakrishna[3]

[1, 3] Materials Research Centre, Indian Institute of Science, Bangalore 560012
(E-mails: garani@mrc.iisc.ernet.in, jagdish@mrc.iisc.ernet.in)
[2] Laboratoire des Colloides Verres et Nanomateriaux CNRS UMR 5587, Universite de Montpellier II, Place Bataillon, 34095 Montpellier CEDEX 5, France.
(E-mails: matteo.ciccotti@LCVN.univ-montp2.fr)

ABSTRACT

Understanding the intermittent peel process and the accompanying audible noise of an adhesive tape has long remained a mystery. Recently, we proposed a model that provides a basis for understanding the dynamics of the peel front as also the acoustic emission. In the model, the acoustic energy is represented in terms of Rayleigh dissipation functional that depends on the local strain rate. The model offer explanations for several experimental features including the statistics of acoustic signals. It also exhibits rich peel front patterns ranging from smooth, rugged and stuck-peeled configurations; the latter is reminiscent of fibrilar pattern observed in experiments. Even as the model acoustic energy is a fully dynamical quantity, it can be quite noisy for a certain set of parameter values suggesting the deterministic origin of acoustic emission in experiments. In order to verify these results, we have performed experiments to obtain acoustic signals over a wide range of traction velocities. Using standard phase space reconstruction procedure we show the existence of correlation dimension as also a positive Lyapunov exponent for the range of pull speeds from 3.8 cm/s to 6.2 cm/s. The model provides a basis for understanding several features of the experimental signals including the transition from burst type continuous type signal with increasing pull velocity.

Coupled Simulation of Grain Boundary Decohesion and Hydrogen Segregation

Mitsuhiro Itakura, Hideo Kaburaki, Masatake Yamaguchi and Tomoko Kadoyoshi

Fundamental Studies on Technologies for Steel Materials with Enhanced Strength and Functions, Consortium of JRCM (The Japan Research and Development Center for Metals),Center for Computational Science and e-Systems, Japan Atomic Energy Agency, 110-0015 Taito-ku, Japan
(E-mail: itakura.mitsuhiro@jaea.go.jp)

ABSTRACT

We present a modeling framework and simulation results of hydrogen embrittlement at the grain boundary region, in which a finite element model of intergranular crack propagation is constructed by incorporating the microscopic model of hydrogen segregation effect on the grain boundary decohesion. The final aim of the study is to identify the mechanism of delayed failure of welded high-strength steel induced by hydrogen, focusing on the microscopic effect of surface energy reduction by hydrogen segregation. Using the first principles method, we have estimated the surface energy and segregation energy as a function of hydrogen content in a Σ3 grain boundary of iron. From these data, we have derived the cohesive stress-displacement relation for separating two atom planes of the grain boundary. Based on these ab-initio results, we have predicted that segregation of hydrogen to a grain boundary could lead to an embrittlement, and this effect can be enhanced by the segregation of hydrogen to the cracked surface. To confirm these predictions, we have simulated simultaneously a hydrogen segregation and grain boundary decohesion within a framework of finite element method. The result indicates that a critical tensile stress for instantaneous and delayed fracture of hydrogen-charged material is approximately 66% and 33% of that of uncharged material, respectively. This result is strikingly consistent with experimental observations [1].

[1] A.R. Troiano: Transactions of the ASM 52, 54 (1960).

Statistical Models for Planar Crack Propagation

Stefano Zapperi[1], Mikko Alava[2], Phani Nukala[3]

[1]INFM-CNR, S3, Dipartimento di Fisica, Universita di Modena e Reggio Emilia, I-41100, Modena, Italy (stefano.zapperi@unimore.it)
[2]Helsinki University of Technology, FIN-02015, HUT, Finland, (mja@fyslab.hut.fi)
[3]Computer Science and Mathematics Division, Oak Ridge National Laboratory, Oak Ridge, TN 37831-6164 (n2k@ornl.gov)

ABSTRACT

We investigate the effect on the crack front roughness of microcrack nucleation ahead of a propagating planar crack by numerical simulations of the random fuse model. We consider a three dimensional geometry, confining the crack to move along a weak plane. We discuss the effect of the sample thickness on the crack roughness and the strength and compare with continuum models for crack line depinning.
.

A Statistical Approach to High-Temperature Plasticity of Ceramic Polycrystals

Diego Gómez-García[1], Eugenio Zapata-Solvas, Arturo Domínguez-Rodríguez

[1]Departamento de Física de la Materia Condensada, Instituto de Ciencia de Materiales, centro mixto CSIC-Universidad de Sevilla, apartado 1065, 41080 Sevilla, SPAIN. (E-mail: dgomez@us.es)

ABSTRACT

. From a fundamental viewpoint, high-temperature plasticity is likely to be the result of grain boundary sliding of grains under stationary conditions. More particularly, all existing models are based upon lattice or grain boundary dislocation activity, despite the fact that such activity has never been observed in many systems, particularly ceramics. This paper outlines a new model accounting for high-temperature plasticity without dislocation activity.

1. Introduction

A consistent theory of high-temperature plasticity must give account for the following facts:

1- Deformation must proceed without variation of microstructure. This is an experimental fact.
2- The stress exponent is reported to be equal to 1 in many polycrystalline systems, whereas it is commonly equal to 2 in others [1]. Quite recently, it has been reported repeatedly a transition from a value of 2 towards 1 when the flow stress or the grain size increases [2,3].
3- The grain size exponent is usually found to be equal to 2 or 3 in most cases, although values of 1 are reported in some of them.

Since the second half of the last Century, a vast number of publications have proposed different high-temperature deformation mechanisms. Reviews on the different models are reported in literature [2,3]. In non-pure systems, the glassy-phase is proved to play a central role as a medium for species solution, migration and ulterior grain boundary precipitation. A review on all models developed for non-pure materials is made by Meléndez et al [4].

When focused on pure (glassy-phase free) materials, nowadays, two main models are invoked: the first one is the Ball-Hutchinson model [5]. This one states that deformation is due to intergranular dislocation glide accommodated by dislocation climb at grain boundaries. Such model has revealed to be applicable in many metallic and non-metallic systems [6], in which Frank-Read source activation is energetically favourable. However, it is obviously inconsistent with the absence of dislocation activity in many ceramic systems.

Another classical model which has been considered until now is the one proposed by Ashby-Verrall [7]. Such model proposes a topological mechanism for grain boundary sliding

with two sequential processes: grain slide is followed by accommodation through diffusion species along the grains. Unfortunately this model seems to be inconsistent with experiments.

A new model is outlined here [8]. This model disregards for dislocation activity, and it is capable for a consistent explanation of the values of the stress exponent in those systems where dislocation activity does not exist.

2. Theory

Let us consider a cylindrical-shaped polycrystalline specimen with mean grain size d. We also admit that grain motion is uncorrelated at times that are large with respect to the time scale of a single event.

Statistically, a mean flight time, $\Delta\tau_S$, can be associated to pure shear motion. This deformation is accommodated through lattice or grain diffusion processes during a mean characteristic time $\Delta\tau_D$. In what follows, use is made of the ratio of these two characteristic times, $\beta = \Delta\tau_s / \Delta\tau_D$.

During a given time Δt, the effective time for shear displacement (Δt_{eff}) is only the weighted average of the pure shear and pure accommodation characteristic times, i.e.:

$$\Delta t_{eff} = \Delta t \frac{\Delta\tau_s}{\Delta\tau_s + \Delta\tau_D} \tag{1}$$

The mean displacement per grain ($\overline{w}$) during a time interval Δt must be:

$$\overline{w} = \frac{d}{\Delta\tau_s}\Delta t_{eff} = d\frac{\Delta t}{\Delta\tau_S + \Delta\tau_D} \tag{2}$$

The increment of section $d\dot{S}$ during that time interval would be given by:

$$d\dot{S} = 2\pi R \frac{\overline{w}}{\Delta t} N_{shear} \tag{3}$$

Where N_{shear} is the number of pure-shear events under steady-state regime.

Now it is possible to find a closed expression for (2) in terms of the stress and temperature if a calculation of $\Delta\tau_S$ and $\Delta\tau_D$ is carried out. Regarding the second one, it is straightforwardly obtained from the diffusion theory [8]:

$$\Delta\tau_D = \frac{d^2}{\sigma\Omega D_{eff}} kT \tag{4}$$

Where Ω is the atomic volume of the accommodation-controlling diffusing species and D_{eff} is the effective diffusion coefficient along the several diffusion paths.

After straightforwardly algebra, one can conclude that the steady state strain rate $\dot{\varepsilon}$ can be expressed as:

$$\dot{\varepsilon} = 2\frac{\beta}{(1+\beta)^2}\frac{\sigma\Omega}{kTd^2}D_{eff} \tag{5}$$

The value of β can be calculated provided an expression for Δτs in function of temperature and the stress is available. Analytical estimates prove that β is proportional to the applied stress, since the glide time has such dependence [8].

3. Discussion and experimental assessment

According to Eqn. (5) a parabolic dependence of the strain rate versus the applied stress should expected provided the value of β<<1. Such condition is consistent with the high-temperature domain. A careful analysis of the stress and temperature dependence of the theoretical law given by Eqn. (5) is beyond the scope of this paper, and such analysis is thoroughly carried out in [8].

Several experimental assessments are made in [8]. In particular, experimental data from different creep tests carried out in yttria tetragonal zirconia polycrystals were fitted to Eqn. (5). Such fit is reproduced in Fig.1 and it is in good agreement with the dependency exhibited in such equation.

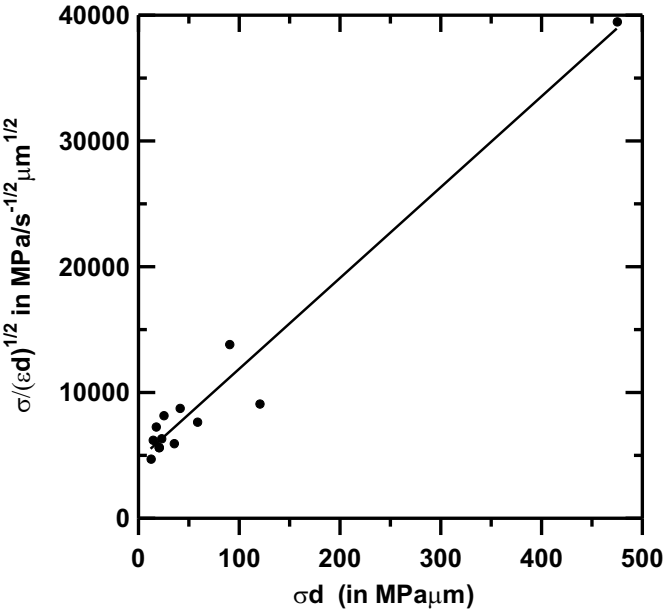

Figure 1: Numerical fit of experimental data in yttria tetragonal zirconia polycrystals deformed at 1350ºC as reported in [8]. In such reference it is proved that such fit is consistent with the prediction made in Eqn. (5).

The main implications of the discussed model can be outlined as follows:
1-A parabolic dependence of the strain rate versus the applied stress is predicted provided $\beta << 1$. Such condition is readily expected in most systems in the high-temperature domain.
2-The temperature dependence of the strain rate is complex and there is not a simple Arrhenius dependence from which an activation energy could be measured. It puts forward in a stress dependence of an 'effective' activation energy for plasticity. Further details are reported in [8].

4. Conclusions

A model for high-temperature superplasticity explaining is developed. The model is based on grain boundary dislocation-free mechanism**.** Experimental validation is briefly commented.

Acknowledgements

The authors would like to gratefully acknowledge fruitful discussions with Prof. O. A. Ruano from 'Centro Nacional de Investigaciones Metalúrgicas (CENIM)' Spain. Financial support is provided by Fund awarded by the Spanish authorities: MAT2006-10249-C02-02.

References

[1] R. C. Gifkins and T. G. Langdon, "Comments on theories of structural superplasticity", Mat. Sci. and Eng. **36,** 27(1978).
[2] R. C. Gifkins and T. G. Langdon, "Further comments on theories of structural superplasticity", Mat. Sci. and Eng. **40**, 293 (1979).
[3] A. Padmanabhan, "A reply to comments on theories of structural superplasticity", Mat. Sci. and Eng. **40**, 285 (1979).
[4] J.J Meléndez-Martínez and A. Domínguez-Rodriguez, "Creep in silicon nitride", Prog. Mat. Sci. **49** nº1, 19 (2004).
[5] A. Ball and M. M. Hutchinson, "Superplasticity in the aluminium-zinc eutectoid", J, Mat. Sci. **3**, nº1, 1 (1969).
[6] O. A. Ruano, J. Wadsworth and O. D. Sherby, "Deformation of fine-grained alumina by grain boundary sliding accommodated by slip", Acta mater. **51**, 3617 (2003).
[7] M. F. Ashby and R. A. Verrall, "Diffusion-accommodated flow and superplasticity". Acta mater. **21**, 149 (1973).
[8] D. Gómez-García, E. Zapata-Solvas, A. Domínguez-Rodríguez and L. P. Kubin, "A model for difusión-driven plasticity in ceramic polycrystals", submitted to Phys. Rev. B.

Statistical Behavior of Internal Stress in 2D Dislocation Assemblies

Isabel Corominas[1], **Lasse Laurson**[2], **Mikko Alava**[2] **and M. Carmen Miguel**[1]

[1]**Departament de Física Fonamental, Facultat de Física, Universitat de Barcelona, Avda. Diagonal 647, E-08028 Barcelona, Spain**
(E-mail: isabel@ffn.ub.es)

[2]**Laboratory of Physics, Helsinky University of Technology, P.O. Box 1100, 02015 HUT, Finland**

ABSTRACT

In recent years the statistical behavior of plastic deformation has received growing interest. In response to the application of external stress, crystalline materials may deform plastically due to the collective motion of dislocations. The dynamics of these topological defects is governed by kinetic constraints, by elastic long range interactions, as well as by multiplication and annihilation processes at short distances. As a result, intricate dislocation patterns may form and dislocation motion is strongly heterogeneous in space and time, proceeding in the form of plastic avalanches with universal scaling properties.

Building up upon these premises, one of the many interesting features concerning crystalline plastic deformation regards the stress distribution in both jammed and moving dislocation arrangements. Here we present simulation results of a simplified model of plastic deformation in two dimensions where discrete edge-like dislocations may glide along a single slip system, and focus on the statistical analysis of the stress distribution in the resulting dislocation assemblies. We first identify clusters of positive and negative stress and compute its size and geometrical properties for different values of the external stress applied. As we approach a given stress threshold, the distribution of cluster sizes becomes very broad, and we can identify a peak in the corresponding second moment of the distribution. We further analyze the scaling properties of the cluster correlation lengths on approaching this threshold. The analysis of our results allows us to reinterpret previous numerical observations suggesting an underlying dislocation yielding transition in the same model from a different and more clarifying viewpoint.

We acknowledge financial support from the Spanish Ministerio de Educación y Ciencia (FIS 2007-66485-C02-02) and from the Generalitat de Catalunya. IC ackowledges Universitat de Barcelona for financial suport.

Effect of Stacking Fault Energy on Defect of Accumulation in Stainless Steels

Xiaoqiang Li

Nuclear material research department, SCKCEN,Boeretang 200, MOL 2400, Belgium
(E-mail: xiaoqiang.li@sckcen.be)

ABSTRACT

Effect of Stacking Fault Energy on Defect of Accumulation in Stainless Steels X. Li, W. van Renterghem, A. Almazouzi SCK.CEN, Reactor Materials Research Department, LHMA, Boeretang 200, 2400-Mol- Belgium Stacking fault energy (SFE) is considered as a key parameter of materials influencing IASCC in nuclear light water reactor (LWR), because it plays an important role in every process of plastic deformation, work hardening and creep behaviors. This paper concentrates on the characterization of irradiation damage of 3 model alloys with different SFEs under controlled irradiation conditions. The detail information of the microstructures, irradiation induced small defect clusters, including their types, natures, densities and size distributions, are determined and statisticized by the classic and special TEM diffraction techniques. The results are good agreement with other literatures. It is shown that, the stacking fault energy (SFE) has strong effect on defect accumulation of irradiated stainless steels. Because the SFE has strong effect on both the deformation mechanisms and irradiation induced defect accumulation, it is thus expected that the susceptibility of 3 model alloys with different SFE to IASCC will be different.

Scaling of the Non-Affine Deformation of Random Fiber Networks

R.C. Picu, H. Hatami-Marbini

Department of Mechanical, Aerospace and Nuclear Engineering, Rensselaer Polytechnic Institute, Troy, NY 12180 (E-mail: picuc@rpi.edu, hatamh@rpi.edu)

ABSTRACT

Random fiber networks are broadly encountered in nature. Examples of such systems are the cytoskeleton, collagen networks in cartilage, paper, filters etc. Their deformation is dictated by the fiber properties and arrangement and is non-affine on multiple scales. The "homogenized" behavior on the macroscopic (system level) scale is determined to a large extent by the degree of non-affinity. It is currently believed that denser networks and networks in which the fibers have vanishing bending stiffness deform affinely. Here we show that these conclusions depend on the nature of the measure used to probe the non-affinity [1]. If a strain based measure is used, it can be shown that all networks, irrespective of the axial or bending behavior of their fibers are non-affine. The non-affinity decreases with the observation scale following a power law scaling with two regimes: one for length scales smaller than the fiber length, and another for larger length scales. The small length scale scaling appears only when the bending stiffness of the fibers is significant. The two scaling regimes are places in relation with geometrical features of the microstructure.

[1] H. Hatami Marbini, R.C. Picu, "Scaling of nonaffine deformation in random semiflexible fiber networks" Physical Review E, **77**, 062103 (2008).

Acknowledgment: This work was supported by the NSF through grants No. 0310596 and 0303902.

.

Predictions of a continuum dislocation density theory: cell wall and grain boundary evolution in crystals

Yong Chen[1], Woo Song Choi[1], Stefanos Papanikolaou[1], Surachate Limkumnerd[2], and James P. Sethna[1]

Affiliations: [1]Yong Chen, Laboratory of Atomic and Solid State Physics, Cornell University, Ithaca, NY 14853-2501, USA, yc355@cornell.edu; [2]Physics Department, Faculty of Science, Chulalongkorn University, Phayathai Rd., Pathumwan, Bangkok 10330, THAILAND, surachate@sc.chula.ac.th

ABSTRACT

We explore the implications of a recently proposed class of continuum theories of plasticity [1,2] that naturally predict the formation of dislocation walls[2]. By using several finite-difference schemes (ENO-Godunov, Upwind etc.) for simulating the time evolution of wall patterns, we study various dislocation-related phenomena and compare with experimental facts. In particular, we incorporate work hardening via a strongly rate dependent slip, and explore the effects of the resulting grain and cell morphologies. In addition, we investigate different aspects of grain coarsening in an extended continuum theory where the effects of dislocation core energies in the continuum limit are taken into account.

[1] Amit Acharya and Anish Roy, "Size effects and idealized dislocation microstructure at small scales: Predictions of a Phenomenological model of Mesoscopic Field Dislocation Mechanics: Part I", J. Mech. Phys. Solids 54 1687-710 (2006).
[2] Surachate Limkumnerd and James P. Sethna, "Mesoscale theory of grains and cells: crystal plasticity and coarsening", Physical Review Letters **96**, 095503 (2006).

This work currently supported by DOE DE-FG02-07ER45393.

Roughness of Damage Paths and Cavities in Shock Loaded Tantalum

Davis Tonks, John Bingert, Veronica Livescu

Los Alamos National Laboratory, Los Alamos, New Mexico, USA
(E-mail: tonksfam@hotmail.com)

ABSTRACT

Earlier work has shown that incipient ductile spallation damage in Tantalum samples recovered from gas gun experiments exhibits voids connected by regions of localized plastic flow. In a two dimensional cross section, these regions and the voids form paths that have a well defined roughness. Recently, a serially sectioned series has been performed on a sample which illustrates how this roughness develops from the 3D damage field. The sample also exhibits a cavity in some of the cross sections. The roughness properties of the 3D damage field and the cavity, as manifest in the series, will be analyzed to explain the 2D roughness appearing in the cross sections.

Heterogeneities Induced by Dislocation Multiplication in Ice: Experimental and Numerical Evidences

Juliette Chevy[1,2], Paul Duval[1], Marc Fivel[2], Jérôme Weiss[1], Pierre Bastie[3]

[1]Laboratoire de Glaciologie et Géophysique de l'Environnement, 54 rue molière, BP96, 38402 St Martin d'Hères Cedex (juliette.chevy@gmail.com)
[2]Laboratoire Science et Ingénierie des Matériaux et Procédés, 101 rue de la physique, 38402 St Martin d'Hères Cedex (Marc.Fivel@simap.grenoble-inp.fr)
[3]Laboratoire de Spectrométrie Physique, 140 rue de la physique, 38402 St Martin d'Hères Cedex (bastie@spectro.ujf-grenoble.fr)

ABSTRACT

Ice is a hexagonal material with a strong viscoplastic anisotropy that deforms essentially by glide of basal dislocations. Torsion tests performed with the c-axis parallel to the torsion axis and 3D Discrete Dislocation Dynamics simulations suggest dislocation multiplication by a double cross-slip mechanism. This process leads to a plastic activity that is heterogeneous both in time and space. Hard X-ray diffraction experiments and dislocation dynamics simulations reveal a scale-free intermittent flow and a scale-invariant character of the deformation along the sample with long range correlations.

1. Introduction

Ice is a crystalline material with an hexagonal crystallographic structure that exhibits a strong plastic anisotropy: plastic strain essentially develops by glide of basal dislocations. Moreover, when basal glide is active, the strain rate ($\dot{\gamma}$) can be related to the stress (τ) through a power-law relationship: $\dot{\gamma} = B(T)\tau^2$ [1]. In order to study dislocation dynamics responsible for this anisotropy, we perform torsion creep (constant loading) tests on single crystals with the c-axis that fits torsion axis. In that configuration, basal planes are loaded in pure shear, and screw dislocations that accomodates torsion strain are pushed towards the center of the cylinder to form twist boundaries. Therefore, if no other glide system is active, this configuration would lead to a finite strain, contrary to experimental evidence (Fig. 1).

Since the applied momentum does not induce any non basal force component, only internal stresses can be at the origin of non-basal glide. Moreover, as only screw dislocations are needed to accommodate torsion, we suggest a double cross-slip multiplication mechanism by way of prismatic slip to explain the increase with time of the strain rate (Fig. 1). With this assumption, numerical simulations performed by means of a 3D Discrete Dislocation Dynamics (DDD) code show that with this assumption, the plastic flow experimentally observed is well reproduced, as well as the strain rate dependence to the stress.

Internal stresses caused by dislocations decrease as 1/r and lead therefore to long range interactions. Previous work (see e.g. [2] and [3]) has shown that these interactions result in an intermittent heterogeneous plastic flow characterized by a scale-free distribution of dislocation avalanche sizes and locations. We present here characteristics of these spatial heterogeneities evidenced through an original application of hard X-ray diffraction properties and through DDD simulations.

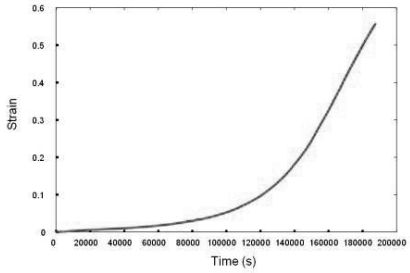

Figure 1. Creep curve for an ice single crystal (Ø=h=43mm) deformed in torsion at -12°C under τ=0.12MPa at cylinder periphery.

2. Experimental data analysis

2.1 The hard X-ray diffraction technique

To investigate heterogeneities along the samples, we carried out hard X-ray diffraction experiments in Institut Laue Langevin (Grenoble, France) on radial slats (height~width~20mm, thickness~2mm) cut from samples deformed in torsion. This technique described in refs [4,5] enables to analyse bulk samples (until several cm of thickness) and is well adapted to study ice deformation because of its very low X-ray absorption. Fig. 2a. is a schematic representation of a diffraction pattern obtained for a good crystal slightly distorted around c-axis. In this figure, the diffraction of basal planes gives an horizontal line (no distorsion) whereas the diffraction of the prismatic planes gives an inclined line. The inclination of the line is directly related to the lattice distorsion around the c-axis. Moreover, each point of the diffracted line is associated with a well defined volume of the sample, it is thus possible to relate the distorion to its position along the sample.

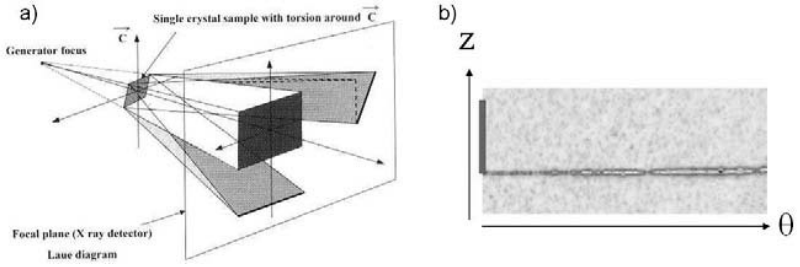

Figure 2. Diffraction pattern a) Schematic representation. b) of the prismatic planes for a highly distorted sample. The thick line represent what would be obtained for a non deformed crystal.

2.2 Strongly deformed samples

In the case of a strongly distorted crystal, the kinematic diffraction theory is valid and the diffracted intensity is proportional to the diffracting volume. Therefore, diffracted intensity reflects the local distortions of the crystal since a less distorted part of the sample corresponds to a larger volume diffracting at the same Bragg angle.

Moreover, the stronger a sample is deformed, the more the prismatic planes are distorted and the more the corresponding relative Bragg angles range will be extended. As for a macroscopically homogeneous deformed sample, a linear relationship exists between the distortion and its location in the sample, a remarkable feature is that by increasing the deformation of the sample, we increase the spatial resolution. For example, a sample with ∅=h=43mm deformed at 40% (equivalent to a ~45° torsion angle) offers a spatial resolution better than 10μm. Fig. 2b is an example of diffraction pattern for such a deformed sample.

Thanks to these two properties, we have access to the local distortion repartition along the sample through diffracted intensity.

2.3 Statistical analysis

Since samples are highly distorted, several diffraction patterns obtained by rotating the sample stage are needed to reconstruct the whole distortion. In order to avoid the introduction of a periodicity induced by this reconstruction, we first remove from the signal trends inherent to the experimental procedure. First, we subtract to the signal the background that is due to the diffusion of the direct beam. We also get rid of the evolution of the diffracted intensity with the Bragg angle (θ) that varies as θ^2.

From this signal (see Fig. 3a), we calculate its autocorrelation function as well as the corresponding power spectrum (Fig. 3b-c).

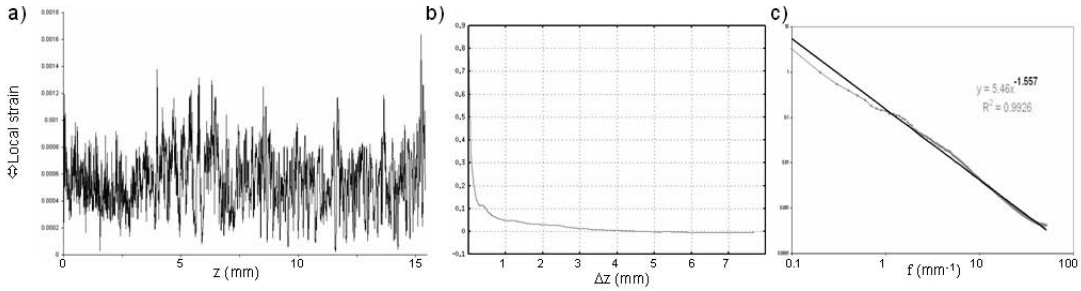

Figure 3. a) Evolution of the diffracted intensity as a function of its position in the sample. b) Autocorrelation function of the same signal. c) Corresponding power spectrum.

This analysis reveals a power law regime of the power spectrum $E(f) \sim f^{-\mu}$ with an exponent $\mu \sim 1.6$, slightly different from what was obtained by X-ray synchrotron topography by [6], and that extends over nearly 3 orders of magnitude. This shows the scale invariance of the local distortions along the sample : these deformation heterogeneities are spatially correlated over large distance (more than 1cm), revealing long range interactions between dislocations accommodating torsion strain.

2. DDD modelling

Torsion creep simulations were performed by means of an edge-screw model initially developped for f.c.c. materials [7] that has been adapted to structure, physical properties and dislocation mobility of ice. Cross-slip of screw dislocations is allowed through a stochastic algorithm that takes into account the applied stress and internal stresses. For calculation time saving reasons, we performed simplified simulations with initially only two planes, each one containing one dislocation source among the six that are possible. From these simulations, we

calculate the displacement fields induced by dislocation motions along a line parallel to the c-axis, representative of the local distortion. A typical profile is presented in fig 4a. From this signal, we calculated the autocorrelation function and the power spectrum given in fig 4b-c. As for the experiments, the spatial repartition of the local lattice distortions is scale invariant and long range correlated. The exponent of the power-law is $\mu \sim 1.5$ that is consistent with experimental results.

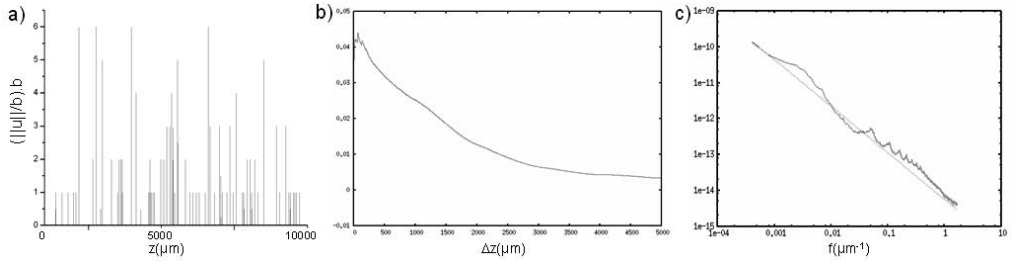

Figure 4. a) Displacement fields along the sample obtained by DDD simulations. b) Autocorrelation function of the same signal. c) Corresponding power spectrum.

3. Conclusions

Both experiments and DDD simulations of the plasticity developed in ice single crystals loaded in torsion creep show that plastic strain is heterogeneous. Scale invariance and long range correlations characterize this heterogeneity. With the configuration of the tests, this can only originate from internal stresses created by dislocations. Long range interactions between dislocations at the micron scale trigger cross-slip events, leading to a self-organization of the dislocations that determines the macroscopical behaviour. The analysis of deformation intermittency is expected to evidence same characteristics and to be correlated with its scale free spatial distribution.

References

[1] P. Duval, M.F. Ashby, I. Anderman, "Rate-Controlling Processes in the creep of polycrystalline ice", J. Phys. Chem., **87**, 4066-4074 (1983).

[2] M.C. Miguel, A. Vespignani, S. Zapperi, J. Weiss, J. R. Grasso, "Intermittent dislocation flow in viscoplastic deformation", Nature, **410**, 667-671 (2001).

[3] J. Weiss, D. Marsan, "Three-dimensional mapping of dislocation avalanches: clustering and space/time coupling", **299**, 89-92 (2003).

[4] P. Bastie, B. Hamelin, "La méthode de Laue refocalisée à haute énergie: une technique d'étude en volume des monocristaux", J. Phys. IV, colloque C4, **6**, 13-21 (1996).

[5] B. Hamelin, P. Bastie, "Méthode de Laue refocalisée à haute énergie: développements récents", J. Phys. IV France, **8**, 3-8 (1998).

[6] M. Montagnat, J. Weiss, J. Chevy, P. Duval, H. Brunjail, P. Bastie, J. Gil Sevillano, "The heterogeneous nature of slip in ice single crystals deformed under torsion", Phil. Mag., **86**, 4259-4270 (2006).

[7] M. Verdier, M. Fivel, I. Groma, "Mesoscopic scale simulation of dislocation dynamics in fcc metals: Principles and applications", Modelling Simul. Mater. Sci. Eng., **6**, 755 (1998).